Science AAAS

Submitted Manuscript: Confidential

Title: Remobilization of crustal carbon may dominate volcanic arc emissions

Authors: Emily Mason[1], Marie Edmonds[1,*], Alexandra V Turchyn[1]

Affiliations:

[1] Department of Earth Sciences, University of Cambridge, Downing Street, Cambridge CB2 3EQ

*Correspondence to: marie.edmonds@esc.cam.ac.uk.

Abstract: The flux of carbon into and out of Earth's surface environment has implications for Earth's climate and habitability. We compiled a global dataset for carbon and helium isotopes from volcanic arcs and demonstrated that the carbon isotope composition of mean global volcanic gas is considerably heavier, at -3.8 to -4.6 ‰, than the canonical Mid-Ocean-Ridge Basalt value of -6.0 ‰. The largest volcanic emitters outgas carbon with higher $\delta^{13}C$ and are located in mature continental arcs that have accreted carbonate platforms, indicating that reworking of crustal limestone is an important source of volcanic carbon. The fractional burial of organic carbon is lower than traditionally determined from a global carbon isotope mass balance and may have varied over geological time, modulated by supercontinent formation and breakup.

One Sentence Summary: Reworking of crustal carbon dominates volcanic arc outgassing, decreasing the estimate of fractional organic carbon burial.

Main Text:

The core, mantle and crust contain 90% of the carbon on Earth (*1*), with the remaining 10% partitioned between the ocean, atmosphere and biosphere. Due to the relatively short

residence time of carbon in Earth's surface reservoirs (~200,000 years), the ocean, atmosphere and biosphere may be considered a single carbon reservoir on million-year timescales. Carbon is removed from the surface reservoir through formation and deposition of carbonate minerals and organic carbon; and added through volcanic and tectonic carbon outgassing. In the pre-industrial era, volcanic outgassing at arc, rift, and intra-plate areas through vents or diffuse degassing sourced up to 90% of Earth's surface carbon (*2, 3*). The remaining carbon came from tectonic regions, through metamorphic decarbonation of carbon-bearing rocks (*4*) and from the underlying mantle (*5*). While we can account for all of the sources of surface carbon, the origin of carbon coming from volcanic arc outgassing is a fundamental yet unanswered question. The amount of carbon derived from the subducting slab compared to the overlying crust is poorly constrained, but has implications for the amount of carbon returned to Earth's deep interior (*6*) and alters interpretations of the variations in arc volcanic CO_2 flux (*7*).

Determining the cycling of carbon between the surface reservoir and the mantle is important as imbalances greatly influence the amount of total carbon at Earth's surface, which in turn impacts atmospheric pCO_2 and surface temperature. During subduction, carbon-bearing sediments devolatilize (*8*) and carbon-bearing minerals may dissolve into fluids (*6, 9*). Carbon can be transported via primary melts to overlying volcanoes, or reprecipitated in the mantle lithosphere beneath the arc (*6*). Receiving less consideration in the literature is the shallow crustal accretionary carbon cycle, which also can shuffle carbon between different reservoirs (*10, 11*) (**Fig. 1**). Mature continental crust contains three orders of magnitude more carbon than the oceans and atmosphere due to the accretion and assimilation of carbonate platforms from past oceans (*11*). Carbon-rich fluids derived from carbonates can be assimilated into crustal magmatic intrusions, resulting in high-carbon magmas that increase the carbon-outgassing flux from the

volcano. In some arcs, this shallow "crustal" carbon cycle dominates over the deeper "subduction" carbon cycle, such that, to balance downgoing carbon with outgassing carbon, most of the carbon contained within sediments on downgoing slabs must be returned to the deep mantle. The return of slab carbon to the deep mantle is predicted by thermodynamic studies of metamorphic decarbonation (*12*); by observations of isotopically light carbon in diamonds, interpreted to be formed from the recycling of organic carbon associated with subduction (*13*); and by the relative stability of our atmosphere over geological time, which, owing to its small size relative to the Earth's interior, requires that inputs (via volcanoes) must approximately balance outputs (by subduction).

Global isotopic mass balance models help constrain Earth's surface carbon cycle over geological time. These model often assume a constant carbon isotope composition reflecting the typical mantle range of around -6‰ (*14-17*). The burial of organic carbon allows removal of carbon, along with electrons, from the surface reservoir allows progressive oxygenation of the planet (*18*). The fractional organic carbon burial flux, which is the amount of carbon buried as organic carbon, is determined by measuring the carbon isotope composition of carbonate minerals preserved as limestone over time. However, if the assumption of a constant $\delta^{13}C$ of the input is incorrect this has cascading effects on the calculated fraction of carbon buried as organic carbon and other carbon reservoir estimates over geologic time.

We compiled a global dataset for carbon and helium isotopic composition of volcanic gases in arcs and evaluated if assimilation of carbon from overlying crustal carbonates could dominate the global arc volcanic carbon flux. We identified arcs for which this mechanism may dominate the carbon flux. We found a much larger impact of crustal carbonates on the carbon budget, which requires reinterpretation of the global carbon isotope mass balance throughout

Earth history. This has direct implications for the fractional burial of organic carbon (*19, 20*) through geological time.

We can use carbon isotopes, combined with other geochemical tracers (helium isotopes), to determine the origin of carbon in volcanic gases as distinct carbon isotopic compositions characterize carbon sources (*21, 22*) (**Fig. 1**). Delta notation ($\delta^{13}C$) reports carbon isotopes as the ratio of the heavy ^{13}C isotope relative to the lighter ^{12}C isotope relative to a standard in units of parts per thousand. CO_2 released at arc volcanoes derives from one of three sources: (i) mantle (-6.0 ± 2.0 ‰) (*23-27*), (ii) sedimentary organic carbon (<-20 to -40 ‰) and (iii) carbonate carbon (~0‰) (*21*). The $^3He/^4He$ ratio is a geochemical tracer of the relative contributions of magmatic and crustal components to volcanic gases. ^3He is a conservative primordial stable isotope incorporated into the Earth during initial accretion and subsequent accumulation of late veneer material and the amount on Earth is not increasing. Crustal production of ^4He via the decay of uranium and thorium will decrease $^3He/^4He$, providing a strong indicator that the magma has interacted with fluids derived from silicate material in the overlying crust. The isotopic composition of helium is quoted as R/R_A, which is the $^3He/^4He$ in the sample (R), normalized to that in the atmosphere ($R_A = 1.38 \times 10^{-6}$). The canonical MORB-He isotope range is 8±1 R_A (*28*), with the mean ratio for volcanic arcs 5.4±1.9 R_A (*29*). R/R_A higher than the canonical MORB range are ascribed to an undegassed mantle reservoir and is typical of most ocean island basalts (e.g. Hawaii, Iceland, Galapagos) (*30*). $CO_2/^3He$ ratios are a sensitive tracer of carbon source in volcanoes when combined with the $\delta^{13}C$ of the volcanic gas (*21*). Arcs typically have higher $CO_2/^3He$ than MORB, due to the addition of either slab- or crustal-derived carbon (*21*), although it is difficult to distinguish between these sources based on ^3He and $\delta^{13}C$ alone (*22*). $CO_2/^3He$ ratios for volcanic arc gases indicate the mixing of magmatic and sedimentary/crustal

sources of CO_2 and are up to 100 times higher than the mantle range (*21, 31, 32*). Here we suggest that high $CO_2/^3He$ and $\delta^{13}C$ of volcanic gases (*21*), combined with a low R/R_A, provides strong evidence for carbon being derived from the overlying crust as opposed to the downgoing slab.

Our compilation of carbon and helium isotope data (**Fig. 2**) (*22*) for volcanic arc gases allows us to discriminate carbon sources and in doing so, determine the $\delta^{13}C$ of modern volcanic arc gas. Our result challenges the fundamental assumption that $\delta^{13}C$ of volcanic CO_2 has been invariant over geological time. Carbon isotope ratios are available for most arcs worldwide (*21*) (**Table S2**), but some arcs have little or no data. We did not find a systematic variation of $\delta^{13}C$ or R/R_A with sample temperature (*22*). Many arcs emit carbon with a higher $\delta^{13}C$ than the typical mantle range (**Fig. 2**), most notably Italy (*33-35*), the Central American Volcanic Arc, Indonesia (Sangihe and Java-Sunda-Banda) and Papua New Guinea *(22)*. Arcs located in the northern Pacific such as Japan and Kuril-Kamchatka release CO_2 with a $\delta^{13}C$ that lies predominantly within the mantle range. The Cascade and Aleutian Arcs outgas carbon that falls within or lower than the typical mantle $\delta^{13}C$ range and He with R/R_A values consistently within the mantle range. A recent study has linked the $\delta^{13}C$ of volcanic gases emitted along the Aleutian arc with the organic sediment flux into the subduction zone (*7*). A cross plot of carbon and helium isotope data (**Fig. 3**) identifies those arcs whose volcanic CO_2 output is dominated or influenced strongly by crustal carbon assimilation: Indonesia – East Sunda/Banda; the Italian Campanian Magmatic Province (i.e. Vesuvio and Solfatara); and the Andes – Ecuador, Peru and Northern Chile.

In order to estimate a global average $\delta^{13}C$ for gases released at volcanic arcs, we must weight $\delta^{13}C$ by CO_2 flux. Estimating global volcanic CO_2 fluxes is a non-trivial problem (*36*). We cannot measure CO_2 fluxes directly due to the high concentration of CO_2 in the background

atmosphere and the absorption interference in the UV or IR. Estimates instead are usually derived by combining the flux measurement of SO_2 with the ratio CO_2/SO_2 in volcanic gas emission compilations (*7, 37, 38*). Arcs currently represent between 30% and 63% of the total volcanic (arc + mid-ocean ridge + intra-oceanic hotspot) outgassing flux (*39*). We do not show intra-continental hotspots e.g. Yellowstone (*40*) and rifts because of poorly constrained fluxes. Intra-continental rifting, e.g. East Africa, may generate a relatively large CO_2 flux, although the absolute number depends on scaling up from a relatively narrow temporal window and a limited number of sampling locations (*41*). Diffuse degassing may equate to 50% of the passive volcanic CO_2 flux from arcs (*2*), thereby enhancing the contribution of arcs to the global volcanic CO_2 budget. We do not take account of tectonic fluxes of CO_2, which are not well known. We used these fluxes, combined with median $\delta^{13}C$, to calculate the average $\delta^{13}C$ of volcanic gases released today (**Table S4**) (*22*). The non-weighted global arc mean $\delta^{13}C$ is -4.3±2.6‰ (with a median value of -3.8‰). After weighting the median arc values for CO_2 flux at each arc, the global arc average $\delta^{13}C$ is -2.8 to -3.3 ± 0.5‰ (with missing arcs assigned an average $\delta^{13}C$ of -3.0 ‰ for the lower end estimate and -5.0‰ for the higher end). These estimates yield mean global volcanic outgassing carbon compositions of -3.8 to -4.6‰, assuming that arcs represent 33 to 63% (*39*) of the total volcanic input to the atmosphere-ocean system (**Table S4**) (*22*), with mid-ocean ridges accounting for much of the remainder. The volcanic arcs with the highest CO_2 fluxes also have a higher $\delta^{13}C$, suggesting that assimilation and outgassing of crustal carbon may dominate global volcanic CO_2 fluxes (**Fig. 4**).

The carbon isotope signature of volcanic gases reflects their source (organic carbon, limestone, crust, mantle; **Fig. 1**), but may also be modified by carbon isotope fractionation during magma degassing, assimilation of near-surface organic carbon and precipitation of calcite

in the sub-surface geothermal or hydrothermal systems beneath volcanoes (*22*). The high $\delta^{13}C$ of volcanic gases, the high proportions of radiogenic helium, and the mature, continental nature of the overlying crust (*10, 11*) all point to outgassed carbon being sourced dominantly from crustal limestones for a subset of arcs (Central America, Aegean, Papua New Guinea, Indonesia, parts of the Andes). The limestones may be remnants of accreted carbonate platforms. Magma geochemistry provides additional evidence supporting substantial interaction of these magmas with the crust (*22*). Although we recognize that the carbon isotopic composition of volcanic gases may be influenced by a range of factors (*22*), we suggest that crustal carbonate assimilation is a key parameter controlling both the magnitude of the CO_2 flux and its carbon isotope composition in the arcs that dominate global carbon outgassing. If a large fraction of the outgassed carbon is sourced from the overlying crust in some arcs, the implication is that a larger proportion of subducted carbon may return to the deep mantle, as predicted by models of metamorphic decarbonation (*8, 12, 42*).

The global carbon isotope mass balance describes the burial of organic carbon as a fraction of total carbon burial (*f*) through the balance of an exospheric carbon input ($\delta^{13}C_{in}$) and organic carbon ($\delta^{13}C_{org}$) and carbonate carbon ($\delta^{13}C_{carb}$) outputs.

$$\delta^{13}C_{in} = \delta^{13}C_{org} f_{org} + \delta^{13}C\left(1 - f_{org}\right) \qquad \text{(eq. 1)}$$

Ultimately the goal is to solve this equation for f_{org} which allows us to resolve changes in organic carbon burial and thus the redox balance of Earth's surface. In practice, only the $\delta^{13}C_{carb}$ is measured in limestone across a stratigraphic interval. The value for the organic carbon

endmember $\delta^{13}C$ composition is assumed to be 25 to 27‰ lower than the $\delta^{13}C_{carb}$ due to carbon isotope fractionation during photosynthesis. The volcanic input value is usually set at the assumed 'bulk Earth' value, between -5 and -6‰; changing this value ($\delta^{13}C_{in}$) impacts the calculated fractional organic carbon burial. For example, an increase of $\delta^{13}C_{in}$ from ~-5‰ to ~-4.1‰ (**Table S4**) (*22*), decreases the modern f_{org} from ~20% to ~15% if volcanic arcs supply about half of the CO_2 flux to the surface environment (Fig. S5) (*22*).

We suggest that fractional organic carbon burial may be a smaller part of the total carbon removed from the surface of the planet today than previously assumed, based on our data compilation. A present-day f_{org} lower than 20% (i.e. closer to 15%, see above) can occur by the incomplete oxidation of old carbon (*43, 44*) and a return of a substantial fraction of carbon to the ocean-atmosphere system as methane (*45*). This mechanism may explain the discrepancy noted between f_{org} from isotope mass balance (0.19-0.34) and from inventory mass balance (how much sedimentary carbonate is present, 0.10-0.17) (*44*). Our f_{org} (0.15) falls within the range quoted for the inventory mass balance and may be a more reasonable estimate of fractional organic carbon (f_{org}) burial today.

It is likely that the $\delta^{13}C$ of the volcanic input, and thus the overall calculation of f_{org} has varied over the Earth history. Broadly, it has been proposed that transitions between continental-arc dominated and island-arc dominated states, related to the amalgamation and dispersal of continents through Earth history, have the potential to influence atmospheric pCO_2 (*46*). During supercontinent break-up, continental arcs dominate over island arcs. Present-day subduction zones are dominated by island-arcs compared to other periods in Earth's past (e.g. during the Cretaceous, where continental arcs have been shown to be as much as 200% longer than today

(*10, 11*). With continental arcs showing particularly high $\delta^{13}C$ (due to contamination by crustal carbonates), the volcanic $\delta^{13}C$ input during continental-arc dominated periods, often associated with the closing of ocean basins and the breakup of supercontinents, has the potential to be substantially higher than today. We see a prime example of this in the Cretaceous, when overall high $\delta^{13}C$ of marine carbonates has been linked to increased organic carbon burial, and by proxy increased atmospheric oxygen; this has been linked to the evolutionary radiation of mammals (*47*). A substantially higher $\delta^{13}C$ of arc volcanoes associated with the closing of the Tethys Ocean at this time would require a reinterpretation of this record. Furthermore, over Earth history with the breakup of two supercontinents (Kenorland, at 2.1 Ga and Rodinia at 800 Ma) there is sustained high $\delta^{13}C$ measured in marine limestones; both of these high $\delta^{13}C$ are associated with increases in atmospheric oxygen. It is unlikely that a high $\delta^{13}C$ of volcanic CO_2 alone can account for excursions to sustained $\delta^{13}C_{carb}$ as high as +10‰ because the $\delta^{13}C$ input required to produce such values is unreasonable in the context of the highest $\delta^{13}C$ of volcanic CO_2 released today (*22*). However, at higher f_{org} (>0.15) the $\delta^{13}C$ of the volcanic input required for excursions to $\delta^{13}C_{carb}$ = +5‰ is more reasonable, at 0 ± 1‰. We suggest that some of these excursions in $\delta^{13}C$ of carbonate minerals may result from increased $\delta^{13}C$ of the outgassed carbon accompanying continental volcanism during supercontinent breakup due to crustal carbonate assimilation.

References

1. R. Dasgupta, M. M. Hirschmann, The deep carbon cycle and melting in Earth's interior. *Earth and Planetary Science Letters* **298**, 1-13 (2010).
2. M. R. Burton, G. M. Sawyer, D. Granieri, Deep carbon emissions from volcanoes. *Rev. Mineral. Geochem* **75**, 323-354 (2013).
3. N.-A. Mörner, G. Etiope, Carbon degassing from the lithosphere. *Global and Planetary Change* **33**, 185-203 (2002).
4. M. Bickle, Metamorphic decarbonation, silicate weathering and the long‐term carbon cycle. *Terra Nova* **8**, 270-276 (1996).

5. G. Chiodini, C. Cardellini, A. Amato, E. Boschi, S. Caliro, F. Frondini, G. Ventura, Carbon dioxide Earth degassing and seismogenesis in central and southern Italy. *Geophysical Research Letters* **31**, (2004).
6. P. B. Kelemen, C. E. Manning, Reevaluating carbon fluxes in subduction zones, what goes down, mostly comes up. *Proceedings of the National Academy of Sciences* **112**, E3997-E4006 (2015).
7. A. Aiuppa, T. P. Fischer, T. Plank, P. Robidoux, R. Di Napoli, Along-arc, inter-arc and arc-to-arc variations in volcanic gas CO 2/S T ratios reveal dual source of carbon in arc volcanism. *Earth-Science Reviews*, (2017).
8. D. Kerrick, J. Connolly, Metamorphic devolatilization of subducted marine sediments and the transport of volatiles into the Earth's mantle. *Nature* **411**, 293-296 (2001).
9. J. J. Ague, S. Nicolescu, Carbon dioxide released from subduction zones by fluid-mediated reactions. *Nature Geoscience* **7**, 355-360 (2014).
10. F. K. Johnston, A. V. Turchyn, M. Edmonds, Decarbonation efficiency in subduction zones: Implications for warm Cretaceous climates. *Earth and Planetary Science Letters* **303**, 143-152 (2011).
11. C.-T. A. Lee, B. Shen, B. S. Slotnick, K. Liao, G. R. Dickens, Y. Yokoyama, A. Lenardic, R. Dasgupta, M. Jellinek, J. S. Lackey, Continental arc–island arc fluctuations, growth of crustal carbonates, and long-term climate change. *Geosphere* **9**, 21-36 (2013).
12. P. J. Gorman, D. Kerrick, J. Connolly, Modeling open system metamorphic decarbonation of subducting slabs. *Geochemistry, Geophysics, Geosystems* **7**, (2006).
13. S. B. Shirey, P. Cartigny, D. J. Frost, S. Keshav, F. Nestola, P. Nimis, D. G. Pearson, N. V. Sobolev, M. J. Walter, Diamonds and the geology of mantle carbon. *Rev Mineral Geochem* **75**, 355-421 (2013).
14. D. J. Des Marais, H. Strauss, R. E. Summons, J. Hayes, Carbon isotope evidence for the stepwise oxidation of the Proterozoic environment. *Nature* **359**, 605 (1992).
15. L. R. Kump, Interpreting carbon-isotope excursions: Strangelove oceans. *Geology* **19**, 299-302 (1991).
16. D. P. Schrag, J. A. Higgins, F. A. Macdonald, D. T. Johnston, Authigenic carbonate and the history of the global carbon cycle. *science* **339**, 540-543 (2013).
17. P. F. Hoffman, A. J. Kaufman, G. P. Halverson, D. P. Schrag, A Neoproterozoic snowball earth. *Science* **281**, 1342-1346 (1998).
18. J. M. Hayes, J. R. Waldbauer, The carbon cycle and associated redox processes through time. *Philosophical Transactions of the Royal Society of London B: Biological Sciences* **361**, 931-950 (2006).
19. R. M. Garrels, A. Lerman, Coupling of the sedimentary sulfur and carbon cycles; an improved model. *American Journal of Science* **284**, 989-1007 (1984).
20. R. Berner, S. Petsch, J. Lake, D. Beerling, B. Popp, R. Lane, E. Laws, M. Westley, N. Cassar, F. Woodward, Isotope fractionation and atmospheric oxygen: implications for Phanerozoic O2 evolution. *Science* **287**, 1630-1633 (2000).
21. Y. Sano, B. Marty, Origin of carbon in fumarolic gas from island arcs. *Chemical Geology* **119**, 265-274 (1995).
22. Materials and Methods are available as Supplementary Materials on Science Online.
23. D. J. Des Marais, J. G. Moore, Carbon and its isotopes in mid-oceanic basaltic glasses. *Earth and Planetary Science Letters* **69**, 43-57 (1984).
24. D. Mattey, R. Carr, I. Wright, C. Pillinger, Carbon isotopes in submarine basalts. *Earth and Planetary Science Letters* **70**, 196-206 (1984).
25. M. Javoy, F. Pineau, The volatiles record of a "popping" rock from the Mid-Atlantic Ridge at 14 N: chemical and isotopic composition of gas trapped in the vesicles. *Earth and Planetary Science Letters* **107**, 598-611 (1991).
26. P. Cartigny, Stable isotopes and the origin of diamond. *Elements* **1**, 79-84 (2005).
27. B. Marty, L. Zimmermann, Volatiles (He, C, N, Ar) in mid-ocean ridge basalts: Assesment of shallow-level fractionation and characterization of source composition. *Geochimica et Cosmochimica Acta* **63**, 3619-3633 (1999).
28. D. Graham, Noble gases in MORB and OIB: observational constraints for the characterization of mantle source reservoirs. *Rev Mineral Geochem* **47**, 247-318 (2002).
29. D. R. Hilton, T. P. Fischer, B. Marty, Noble gases and volatile recycling at subduction zones. *Reviews in mineralogy and geochemistry* **47**, 319-370 (2002).
30. K. Farley, E. Neroda, Noble gases in the earth's mantle. *Annual Review of Earth and Planetary Sciences* **26**, 189-218 (1998).
31. Y. Sano, S. N. Williams, Fluxes of mantle and subducted carbon along convergent plate boundaries. *Geophysical Research Letters* **23**, 2749-2752 (1996).

32. Y. Sano, J.-I. Hirabayashi, T. Oba, T. Gamo, Carbon and helium isotopic ratios at Kusatsu-Shirane volcano, Japan. *Applied geochemistry* **9**, 371-377 (1994).
33. G. I. Marziano, F. Gaillard, M. Pichavant, Limestone assimilation by basaltic magmas: an experimental re-assessment and application to Italian volcanoes. *Contr. Mineral. and Petrol.* **155**, 719-738 (2008).
34. G. Chiodini, F. Frondini, F. Ponziani, Deep structures and carbon dioxide degassing in central Italy. *Geothermics* **24**, 81-94 (1995).
35. D. Tedesco, Systematic variations in the 3 He/4 He ratio and carbon of fumarolic fluids from active volcanic areas in Italy: Evidence for radiogenic 4 He and crustal carbon addition by the subducting African plate? *Earth and planetary science letters* **151**, 255-269 (1997).
36. T. P. Fischer, Fluxes of volatiles (H2O, CO2, N2, Cl, F) from arc volcanoes. *Geochemical Journal* **42**, 21-38 (2008).
37. A. Aiuppa, C. Federico, G. Giudice, S. Gurrieri, M. Liuzzo, H. Shinohara, R. Favara, M. Valenza, Rates of carbon dioxide plume degassing from Mount Etna volcano. *Journal of Geophysical Research: Solid Earth (1978–2012)* **111**, (2006).
38. H. Shinohara, A. Aiuppa, G. Giudice, S. Gurrieri, M. Liuzzo, Variation of H2O/CO2 and CO2/SO2 ratios of volcanic gases discharged by continuous degassing of Mount Etna volcano, Italy. *Journal of Geophysical Research: Solid Earth (1978–2012)* **113**, (2008).
39. B. Marty, I. N. Tolstikhin, CO 2 fluxes from mid-ocean ridges, arcs and plumes. *Chemical Geology* **145**, 233-248 (1998).
40. C. Werner, S. Brantley, CO2 emissions from the Yellowstone volcanic system. *Geochemistry, Geophysics, Geosystems* **4**, (2003).
41. H. Lee, J. D. Muirhead, T. P. Fischer, C. J. Ebinger, S. A. Kattenhorn, Z. D. Sharp, G. Kianji, Massive and prolonged deep carbon emissions associated with continental rifting. *Nature Geoscience*, (2016).
42. D. Kerrick, J. Connolly, Subduction of ophicarbonates and recycling of CO2 and H2O. *Geology* **26**, 375-378 (1998).
43. N. E. Blair, R. C. Aller, The fate of terrestrial organic carbon in the marine environment. (2011).
44. L. Derry, Organic carbon cycling and the lithosphere. *Treatise on geochemistry*, 239-249 (2014).
45. G. Etiope, D. Oehler, C. Allen, Methane emissions from Earth's degassing: Implications for Mars. *Planetary and Space Science* **59**, 182-195 (2011).
46. N. R. McKenzie, B. K. Horton, S. E. Loomis, D. F. Stockli, N. J. Planavsky, C.-T. A. Lee, Continental arc volcanism as the principal driver of icehouse-greenhouse variability. *Science* **352**, 444-447 (2016).
47. P. G. Falkowski, M. E. Katz, A. J. Milligan, K. Fennel, B. S. Cramer, M. P. Aubry, R. A. Berner, M. J. Novacek, W. M. Zapol, The rise of oxygen over the past 205 million years and the evolution of large placental mammals. *Science* **309**, 2202-2204 (2005).
48. S. Facq, I. Daniel, G. Montagnac, H. Cardon, D. A. Sverjensky, In situ Raman study and thermodynamic model of aqueous carbonate speciation in equilibrium with aragonite under subduction zone conditions. *Geochimica et Cosmochimica Acta* **132**, 375-390 (2014).
49. Y. Tatsumi, S. Eggins, *Subduction zone magmatism*. (Wiley, 1995), vol. 1.
50. P. Schiano, R. Clocchiatti, L. Ottolini, T. Busa, Transition of Mount Etna lavas from a mantle-plume to an island-arc magmatic source. *Nature* **412**, 900-904 (2001).
51. A. M. Shaw, D. R. Hilton, T. P. Fischer, J. A. Walker, G. E. Alvarado, Contrasting He–C relationships in Nicaragua and Costa Rica: insights into C cycling through subduction zones. *Earth and Planetary Science Letters* **214**, 499-513 (2003).
52. L. A. Jaffe, D. R. Hilton, T. P. Fischer, U. Hartono, Tracing magma sources in an arc‐arc collision zone: Helium and carbon isotope and relative abundance systematics of the Sangihe Arc, Indonesia. *Geochemistry, Geophysics, Geosystems* **5**, (2004).
53. Y. Nishio, S. Sasaki, T. Gamo, H. Hiyagon, Y. Sano, Carbon and helium isotope systematics of North Fiji Basin basalt glasses: carbon geochemical cycle in the subduction zone. *Earth and Planetary Science Letters* **154**, 127-138 (1998).
54. J. P. Chadwick, V. R. Troll, C. Ginibre, D. Morgan, R. Gertisser, T. E. Waight, J. P. Davidson, Carbonate assimilation at Merapi Volcano, Java, Indonesia: insights from crystal isotope stratigraphy. *Journal of Petrology* **48**, 1793-1812 (2007).
55. F. Deegan, V. Troll, C. Freda, V. Misiti, J. P. Chadwick, C. McLeod, J. P. Davidson, Magma–carbonate interaction processes and associated CO2 release at Merapi Volcano, Indonesia: insights from experimental petrology. *Journal of Petrology* **51**, 1027-1051 (2010).

56. M. Van Soest, D. Hilton, R. Kreulen, Tracing crustal and slab contributions to arc magmatism in the Lesser Antilles island arc using helium and carbon relationships in geothermal fluids. *Geochimica et Cosmochimica Acta* **62**, 3323-3335 (1998).
57. A. Pedroni, K. Hammerschmidt, H. Friedrichsen, He, Ne, Ar, and C isotope systematics of geothermal emanations in the Lesser Antilles Islands Arc. *Geochimica et Cosmochimica Acta* **63**, 515-532 (1999).
58. R. Poreda, H. Craig, Helium isotope ratios in circum-Pacific volcanic arcs. *Nature* **338**, 473-478 (1989).
59. R. B. Symonds, R. J. Poreda, W. C. Evans, C. J. Janik, B. E. Ritchie, Mantle and crustal sources of carbon, nitrogen, and noble gases in Cascade-Range and Aleutian-Arc volcanic gases. *US Geological Survey Open-File Report*, 03-436 (2003).
60. E. M. Syracuse, P. E. van Keken, G. A. Abers, The global range of subduction zone thermal models. *Physics of the Earth and Planetary Interiors* **183**, 73-90 (2010).
61. P. Allard, The origin of hydrogen, carbon, sulphur, nitrogen and rare gases in volcanic exhalations: evidence from isotope geochemistry. *Forecasting volcanic events* **1**, 337-386 (1983).
62. D. P. Mattey, Carbon dioxide solubility and carbon isotope fractionation in basaltic melt. *Geochimica et Cosmochimica Acta* **55**, 3467-3473 (1991).
63. D. J. Frost, C. A. McCammon, The redox state of Earth's mantle. *Annu. Rev. Earth Planet. Sci.* **36**, 389-420 (2008).
64. H. Ohmoto, M. Goldhaber. (John Wiley & Sons, New York).
65. J. W. Valley, Stable isotope geochemistry of metamorphic rocks. *Reviews in Mineralogy and Geochemistry* **16**, 445-489 (1986).
66. F. Goff, C. J. Janik, H. Delgado, C. Werner, D. Counce, J. A. Stimac, C. Siebe, S. Love, S. N. Williams, T. Fischer, Geochemical surveillance of magmatic volatiles at Popocatépetl volcano, Mexico. *Geological Society of America Bulletin* **110**, 695-710 (1998).
67. T. M. Gerlach, B. E. Taylor, Carbon isotope constraints on degassing of carbon dioxide from Kilauea Volcano. *Geochimica et Cosmochimica Acta* **54**, 2051-2058 (1990).
68. G. Chiodini, S. Caliro, A. Aiuppa, R. Avino, D. Granieri, R. Moretti, F. Parello, First 13C/12C isotopic characterisation of volcanic plume CO2. *Bull Volcanol* **73**, 531-542 (2011).
69. C. Werner, W. C. Evans, M. Poland, D. Tucker, M. Doukas, Long-term changes in quiescent degassing at Mount Baker Volcano, Washington, USA; Evidence for a stalled intrusion in 1975 and connection to a deep magma source. *Journal of Volcanology and Geothermal Research* **186**, 379-386 (2009).
70. Y. Bottinga, Calculated fractionation factors for carbon and hydrogen isotope exchange in the system calcite-carbon dioxide-graphite-methane-hydrogen-water vapor. *Geochimica et Cosmochimica Acta* **33**, 49-64 (1969).
71. B. Marty, W. F. Giggenbach, Major and rare gases at White Island volcano, New Zealand: origin and flux of volatiles. *Geophysical Research Letters* **17**, 247-250 (1990).
72. Y. A. Taran, C. B. Connor, V. N. Shapar, A. A. Ovsyannikov, A. A. Bilichenko, Fumarolic activity of Avachinsky and Koryaksky volcanoes, Kamchatka, from 1993 to 1994. *Bull Volcanol* **58**, 441-448 (1997).
73. T. P. Fischer, W. F. Giggenbach, Y. Sano, S. N. Williams, Fluxes and sources of volatiles discharged from Kudryavy, a subduction zone volcano, Kurile Islands. *Earth and Planetary Science Letters* **160**, 81-96 (1998).
74. Y. A. Taran, J. Hedenquist, M. Korzhinsky, S. Tkachenko, K. Shmulovich, Geochemistry of magmatic gases from Kudryavy volcano, Iturup, Kuril Islands. *Geochimica et Cosmochimica Acta* **59**, 1749-1761 (1995).
75. P. Allard, Composition isotopique du carbone dans les gaz d'un magma dactique (volcan Usu, Japan). Relation entre le rapport 13C/12C des voltailes et le rapport 87Sr/86Sr de la phase silicate dans le volcanisme d'arc Cr hebd. *Seanc. Acad. Sci., Paris* **293**, 583-586 (1981).
76. H. Sakai, O. Matsubaya, Stable isotopic studies of Japanese geothermal systems. *Geothermics* **5**, 97-124 (1977).
77. P. Allard, C. Jehanno, J. Sabroux, Composition chimique et isotopique des produits gazeux et solides de l'activité éruptive du Krakatau (Indonésie) pendant la période 1978–1980. *Séanc. Sci. Paris* **293**, 1095-1098 (1981).
78. J. Varekamp, R. Kreulen, R. Poorter, M. Bergen, Carbon sources in arc volcanism, with implications for the carbon cycle. *Terra Nova* **4**, 363-373 (1992).
79. P. Allard, Proportions des isotopes 13 C e 12 C du carbone émis à haute température par un dôme andésitique en cours de croissance: le Mérapi (Indonésie). *CR Acad. Sci. Paris, D* **291**, 613-616 (1980).

80. R. Poorter, J. Varekamp, R. Poreda, M. Van Bergen, R. Kreulen, Chemical and isotopic compositions of volcanic gases from the east Sunda and Banda arcs, Indonesia. *Geochimica et Cosmochimica Acta* **55**, 3795-3807 (1991).
81. G. Hammouya, P. Allard, P. Jean-Baptiste, F. Parello, M. Semet, S. Young, Pre-and syn-eruptive geochemistry of volcanic gases from Soufriere Hills of Montserrat, West Indies. *Geophysical Research Letters* **25**, 3685-3688 (1998).
82. L. Ruzié, M. Moreira, O. Crispi, Noble gas isotopes in hydrothermal volcanic fluids of La Soufrière volcano, Guadeloupe, Lesser Antilles arc. *Chemical Geology* **304**, 158-165 (2012).
83. P. Allard, Chemical and isotopic composition of high-temperature gases from the new Andesitic lava dome in the Soufriere of Saint-Vincent (Lesser Antilles). *Comptes Rendus des Seances de l'Academie des Sciences. Serie 2* **293**, 721-724 (1981).
84. T. P. Fischer, T. M. Lopez, First airborne samples of a volcanic plume for δ13C of CO2 determinations. *Geophysical Research Letters* **43**, 3272-3279 (2016).
85. L. G. Kodosky, R. J. Motyka, R. B. Symonds, Fumarolic emissions from Mount St. Augustine, Alaska: 1979–1984 degassing trends, volatile sources and their possible role in eruptive style. *Bull Volcanol* **53**, 381-394 (1991).
86. W. C. Evans, N. G. Banks, L. D. White, Analyses of gas samples from the summit crater. *US Geol Surv Prof Paper* **1250**, 227-231 (1981).
87. D. Bergfeld, W. C. Evans, K. A. McGee, K. R. Spicer, Pre-and post-eruptive investigations of gas and water samples from Mount St. Helens, Washington, 2002 to 2005. *A volcano rekindled: the renewed eruption of Mount St. Helens* **2006**, 523-542 (2004).
88. G. Snyder, R. Poreda, A. Hunt, U. Fehn, Regional variations in volatile composition: Isotopic evidence for carbonate recycling in the Central American volcanic arc. *Geochemistry, Geophysics, Geosystems* **2**, (2001).
89. G. De Leeuw, D. Hilton, T. Fischer, J. Walker, The He–CO 2 isotope and relative abundance characteristics of geothermal fluids in El Salvador and Honduras: new constraints on volatile mass balance of the Central American Volcanic Arc. *Earth and Planetary Science Letters* **258**, 132-146 (2007).
90. J. M. Salazar, P. A. Hernández, N. M. Pérez, G. Melián, J. Álvarez, F. Segura, K. Notsu, Diffuse emission of carbon dioxide from Cerro Negro volcano, Nicaragua, Central America. *Geophysical Research Letters* **28**, 4275-4278 (2001).
91. P. Allard, Composition isotopique du carbone dans les gaz d'un volcan d'arc: le Momotombo (Nicaragua). *CR Acad. Sci. Paris, D* **290**, 1525-1528 (1980).
92. J. L. Lewicki, T. Fischer, S. N. Williams, Chemical and isotopic compositions of fluids at Cumbal Volcano, Colombia: evidence for magmatic contribution. *Bull Volcanol* **62**, 347-361 (2000).
93. T. P. Fischer, N. C. Sturchio, J. Stix, G. B. Arehart, D. Counce, S. N. Williams, The chemical and isotopic composition of fumarolic gases and spring discharges from Galeras Volcano, Colombia. *Journal of Volcanology and Geothermal Research* **77**, 229-253 (1997).
94. N. C. Sturchio, S. N. Williams, Y. Sano, The hydrothermal system of Volcan Puracé, Colombia. *Bull Volcanol* **55**, 289-296 (1993).
95. B. Capaccioni, F. Aguilera, F. Tassi, T. Darrah, R. Poreda, O. Vaselli, Geochemical and isotopic evidences of magmatic inputs in the hydrothermal reservoir feeding the fumarolic discharges of Tacora volcano (northern Chile). *Journal of Volcanology and Geothermal Research* **208**, 77-85 (2011).
96. F. Tassi, F. Aguilera, O. Vaselli, T. Darrah, E. Medina, Gas discharges from four remote volcanoes in northern Chile (Putana, Olca, Irruputuncu and Alitar): a geochemical survey. *Annals of Geophysics* **54**, (2011).
97. F. Tassi, F. Aguilera, O. Vaselli, E. Medina, D. Tedesco, A. D. Huertas, R. Poreda, S. Kojima, The magmatic-and hydrothermal-dominated fumarolic system at the Active Crater of Lascar volcano, northern Chile. *Bull Volcanol* **71**, 171-183 (2009).
98. F. Aguilera, F. Tassi, T. Darrah, S. Moune, O. Vaselli, Geochemical model of a magmatic–hydrothermal system at the Lastarria volcano, northern Chile. *Bull Volcanol* **74**, 119-134 (2012).
99. T. Brombach, S. Caliro, G. Chiodini, J. Fiebig, J. C. Hunziker, B. Raco, Geochemical evidence for mixing of magmatic fluids with seawater, Nisyros hydrothermal system, Greece. *Bull Volcanol* **65**, 505-516 (2003).
100. G. Chiodini, L. Marini, M. Russo, Geochemical evidence for the existence of high-temperature hydrothermal brines at Vesuvio volcano, Italy. *Geochimica et Cosmochimica Acta* **65**, 2129-2147 (2001).

101. G. Capasso, M. Carapezza, C. Federico, S. Inguaggiato, A. Rizzo, Geochemical monitoring of the 2002–2003 eruption at Stromboli volcano (Italy): precursory changes in the carbon and helium isotopic composition of fumarole gases and thermal waters. *Bull Volcanol* **68**, 118-134 (2005).
102. G. Chiodini, F. Frondini, B. Raco, Diffuse emission of CO 2 from the Fossa crater, Vulcano Island (Italy). *Bull Volcanol* **58**, 41-50 (1996).
103. A. Rizzo, M. Liuzzo, M. Ancellin, H. Jost, Real-time measurements of δ 13 C, CO 2 concentration, and CO 2/SO 2 in volcanic plume gases at Mount Etna, Italy, over 5 consecutive days. *Chemical Geology* **411**, 182-191 (2015).
104. K. Koepenick, S. Brantley, J. Thompson, G. Rowe, A. Nyblade, C. Moshy, Volatile emissions from the crater and flank of Oldoinyo Lengai volcano, Tanzania. *Journal of Geophysical Research: Solid Earth* **101**, 13819-13830 (1996).
105. L. Wardell, P. Kyle, A. Campbell, Carbon dioxide emissions from fumarolic ice towers, Mount Erebus volcano, Antarctica. *Geological Society, London, Special Publications* **213**, 231-246 (2003).
106. P. Barry, D. Hilton, E. Füri, S. Halldórsson, K. Grönvold, Carbon isotope and abundance systematics of Icelandic geothermal gases, fluids and subglacial basalts with implications for mantle plume-related CO 2 fluxes. *Geochimica et Cosmochimica Acta* **134**, 74-99 (2014).

Supplementary Materials

Acknowledgments: The data reported in this paper are available in the Supplementary Materials. This study was supported by the Alfred P. Sloan Foundation and the Deep Carbon Observatory. This work was supported by an ERC Starting Investigator Grant (307582) to A.V. Turchyn.

Figures

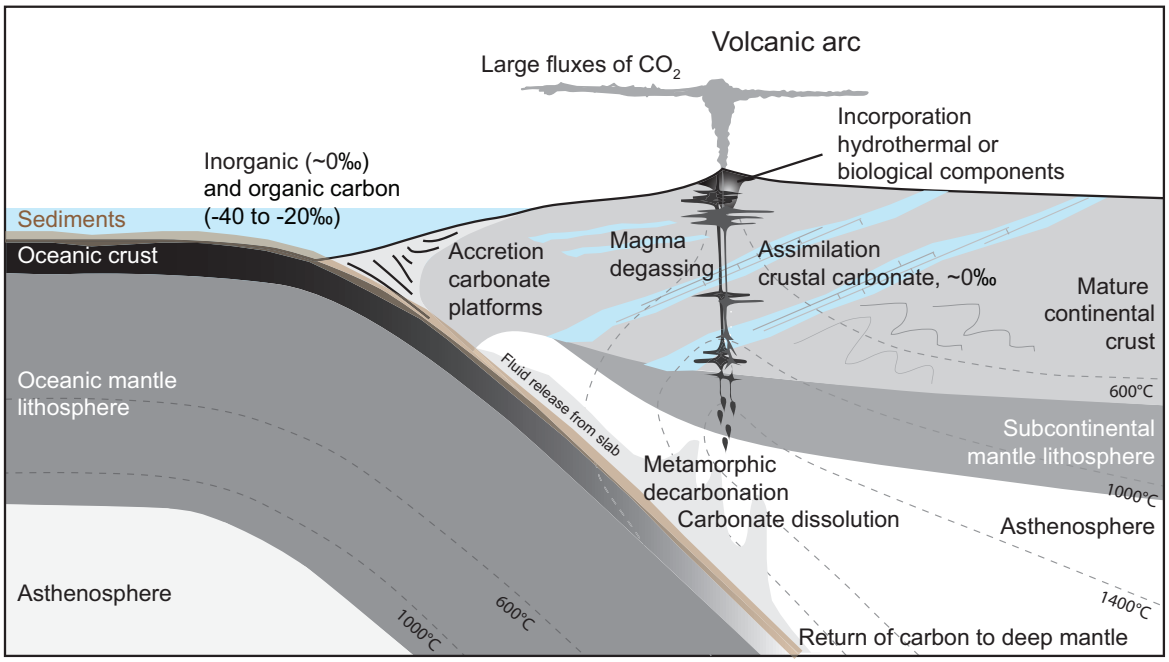

Fig. 1. Schematic diagram to show the possible sources of carbon in a subduction zone volcanic system and the processes which might fractionate carbon isotopes (*22*). Carbon on the downgoing slab is contained within sediments as organic carbon and inorganic carbonate and as inorganic carbonate in the oceanic lithosphere (*6*). Carbon may be remobilized from the slab by metamorphic decarbonation (*12*) or by dissolution into ionic supercritical fluids (*48*); or may be returned to the deep mantle. On ascent through the crust, magmas may interact with crustal carbonate (incorporated into the crust by e.g. accretion of limestone platforms (*11*)), assimilating CO_2-rich fluids, which then outgas during ascent and eruption at the surface. Isotherms are from (*49*).

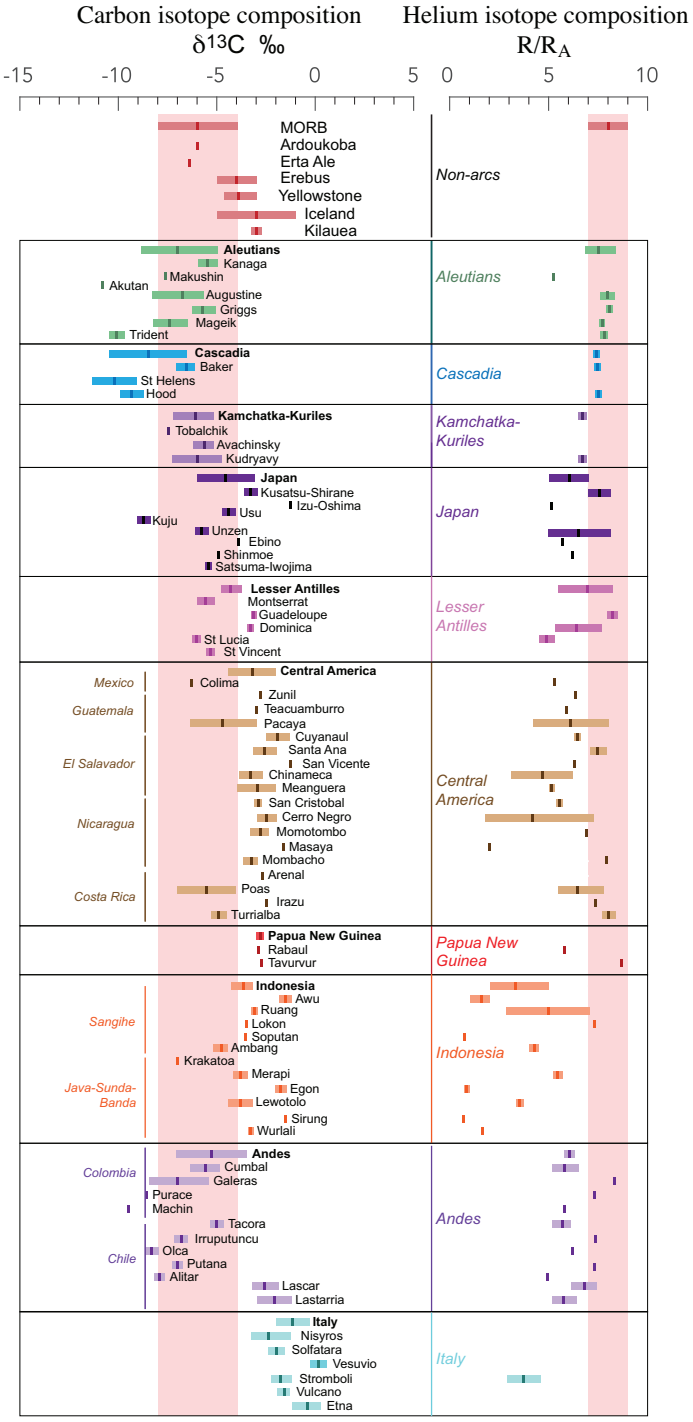

Fig. 2. Carbon and helium isotope compositions of volcanic and fumarolic gases measured at volcanic arcs globally (*22*). Each arc is picked out by different color symbols, labelled with arc

name and in some cases, with country. The mean value is plotted as a darker symbol and the standard deviation lighter in shade on each side. The red shaded columns show the canonical upper mantle values of $\delta^{13}C$ (-6.0 ± 2.5 ‰) and helium isotope ratio $^{3}He/^{4}He$ normalised to the atmospheric value (R/R_A) (8 ± 1). At the top are carbon and helium data for a number of non-arc volcanoes.

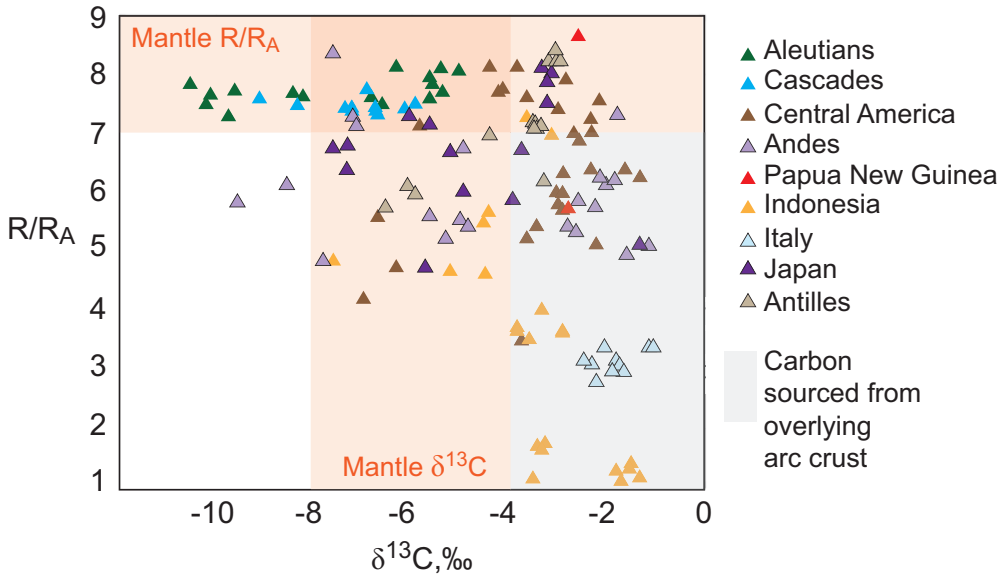

Fig. 3. Plot of helium isotope composition, $^{3}He/^{4}He$, normalized with the same ratio for air (R/R_A) against carbon isotopic composition, in $\delta^{13}C$, ‰, of volcanic arc gases, where both are measured in the same sample (*22*). Mantle ranges are shown as orange panels. The data points are each from an individual arc volcano (*22*) and are colored by volcanic arc; colors as in Fig. 1. Assimilation of crustal material (containing radiogenic He from the decay of U and Th in crustal rocks) and crustal carbonate (supplying isotopically heavy carbon) would push values to the bottom right hand corner of the plot, shaded gray (i.e. high $\delta^{13}C$ and low R/R_A). Plots of $CO_2/^{3}He$ are given in (*22*).

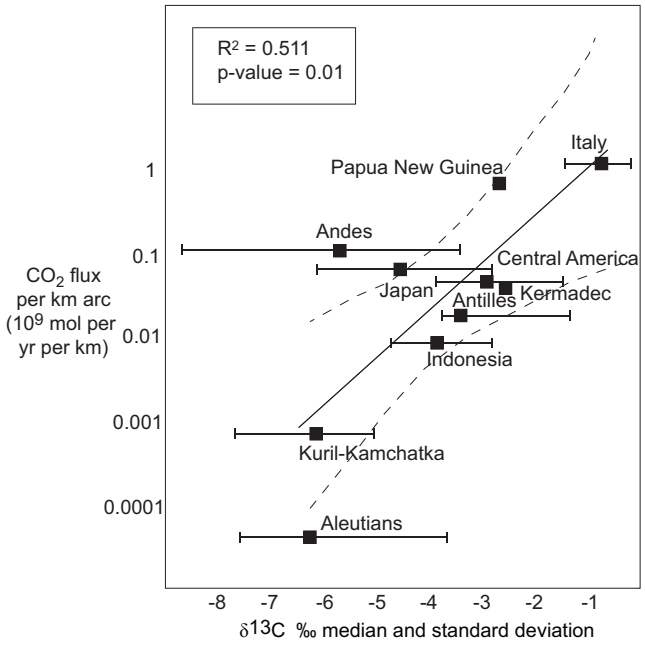

Fig. 4. Plot of CO_2 flux per kilometer of arc length against median carbon isotope composition $\delta^{13}C$ for each arc, in ‰. The horizontal bars represent the standard deviation around a median value. Estimated uncertainties on CO_2 flux are not shown (*22*). The solid grey line is a linear regression and the dashed grey lines are the 95% confidence limits.

Materials and Methods

Data collection and sources

Data presented in this paper are given in **Tables S1** and **S2**, with citations. Samples of gases were collected directly from vents, fumaroles or hot springs. For details of sampling, see individual papers (**Table S1** and **S2**). In general, bubbling gases in the hot springs are introduced by water displacement into glass containers with vacuum stop-cocks. Fumarolic and volcanic gases were directly admitted into containers. After purification, helium was separated and the $^3He/^4He$ ratios were measured with a high precision mass spectrometer. Observed $^3He/^4He$ ratios are calibrated against atmospheric standard gas and are expressed in the R_A notation, where R_A is the atmospheric $^3He/^4He$ of 1.39×10^{-6}. Analytical error of the ratio is in general ± 1%. Absolute contents of He and CO_2 are in general determined using a quadrupole mass spectrometer system (see individual papers). The $^{13}C/^{12}C$ ratios were analyzed by gas-sourced isotope ratio mass spectrometry after separation of CO_2 from other chemical components using e.g. traps held at liquid N_2 and ethanol-dry ice temperature after removal of H_2S e.g. (*21*). Observed $^{13}C/^{12}C$ ratios are expressed in the delta notation, as parts per thousand deviation (per mil, ‰) from the international standard, PDB. The experimental error on the C isotopic ratios are in general ± 0.1‰. The relationship between carbon isotopic composition of the CO_2 in the gas and sample temperature is shown in **Figure S1**.

Weighting of carbon isotope data by flux

To estimate a global average $\delta^{13}C$ for gases released at volcanic arcs, the $\delta^{13}C$ must be weighted by CO_2 flux. CO_2 fluxes are not well constrained. However, it is reasonable to assume that the estimates calculated by (*36*) are representative of the relative magnitudes of arc flux. Therefore, these fluxes, combined with median $\delta^{13}C$, have been used to estimate the average $\delta^{13}C$ of volcanic gases released today (**Table S3**). After weighting the median arc values for CO_2 flux at each arc, as the equation below, a global arc average $\delta^{13}C$ of -3.3±0.5‰ is obtained (if missing arcs have an average $\delta^{13}C$ of -5.5‰) or -2.8 ± 0.5‰ (if missing arcs have an average $\delta^{13}C$ of -3.0‰) (**Table S4**).

$$\delta^{13}C_{global,arc} = \sum_{i=1}^{n} \left(\delta^{13}C_i^{median} \times \frac{C_i^{flux}}{C_{global}^{flux}} \right)$$

When calculating a CO_2 flux-weighted $\delta^{13}C$, there is a clear bias in the data in that the $\delta^{13}C$ of some volcanic arcs is characterized far better than others. An ideal arc $\delta^{13}C$ average would be weighted using fluxes from individual volcanoes. However, few reliable CO_2 fluxes have been published for the volcanoes in this study. Furthermore, within arcs there is often a large discrepancy between the number of data points available for each volcano. Therefore, when trying to calculate a representative mean for the $\delta^{13}C$ of CO_2 released from any one arc, the average arc values will essentially be weighted by the number of data points available. To alleviate this problem, the average global arc $\delta^{13}C$ is calculated using median values.

The standard deviation (±0.5‰) on the average arc $\delta^{13}C$ is a minimum error because uncertainty in the flux estimates (*36*) are not included and arcs with large CO_2 fluxes (i.e. Italy and Papua New Guinea) that contribute significantly to the weighted-average also have small

standard deviations. The standard deviation of the $\delta^{13}C$ for the Papua New Guinea arc is artificially small due to a small number of data points.

Supplementary Text

Additional Explanation of Arc by Arc Data

The $\delta^{13}C$ of CO_2 released at Italian volcanoes is notably higher than other arcs. This has been linked previously to a high degree of crustal carbonate contamination (*33, 34*). A concurrent decrease in R/R_A and increase in $\delta^{13}C$ northward in Italy suggests an increasing degree of crustal contamination, likely from a carbonate source (*35*). However, higher-than-MORB R/R_A values in volcanic products released at Etna have been used to infer the presence of a mantle plume beneath the volcano (*50*) and this may contribute to the northward trend in R/R_A. Large regions of Italy located away from major volcanoes are also degassing, for example the Apennines in central Italy and CO_2 released here also has higher-than-mantle $\delta^{13}C$ (*5*).

The $\delta^{13}C$ data from the Central American Volcanic arc (CAVA) are predominantly higher-than-mantle values, with an average $\delta^{13}C$ of approximately -3‰. On the basis of CO_2, $\delta^{13}C$ and He isotope systematics (*21*) it has been estimated previously that a large proportion (>80%) of CO_2 released on the CAVA is derived from marine subducted carbonates, with a proportion of the fumarolic data plotting on a vector indicating crustal contamination using He and C isotope systematics (*51*). Correlations in the latitudinal trends of the isotopic composition of nitrogen ($\delta^{15}N$) with the ratio Ba/La in recently erupted lavas are consistent with a slab fluid component derived from subducted hemipelagic (containing biogenic and terrigenous) sediments (*36*).

The $\delta^{13}C$ of gases released at the Indonesian volcanoes (Java-Sunda-Banda arc and Sangihe arc) are higher than typical mantle values. In the northern section (Awu volcano) of the Sangihe arc the proportion of carbonate-derived carbon in volcanic CO_2 emissions is >90% while in the southern segment (Ruang and Lokon volcanoes) the proportion is similar to the average value seen at other arcs worldwide (~75%) (*52, 53*). There is a wealth of evidence for crustal carbonate assimilation at a range of Indonesian volcanoes e.g. calc-silicate xenoliths at Merapi and phenocrysts zoned in Sr isotopes (*54, 55*), suggesting that this source may dominate CO_2 emissions in sections of this arc.

Papua New Guinea carbon isotope data have only been published for Rabaul caldera (*31*), with an average of -2.7‰. Since the flux of CO_2 from Papua New Guinea is estimated to be large (*36*) its contribution to the overall $\delta^{13}C$ of volcanic arc CO_2 may be significant.

In the Lesser Antilles, the more southerly islands of St Lucia and St Vincent release volcanic CO_2 with $\delta^{13}C$ within the mantle range, while more northerly islands of Dominca and Guadeloupe release volcanic CO_2 with a higher-than-mantle $\delta^{13}C$. Soufrière Hills Volcano (Montserrat) releases CO_2 at the summit crater with a typical mantle $\delta^{13}C$, however it should be noted that flank fumaroles on Montserrat release CO_2 with a higher $\delta^{13}C$ between -3‰ and -4‰ (*56, 57*).

Arcs located in the northern Pacific such as Japan and Kuril-Kamchatka release CO_2 with a $\delta^{13}C$ that lies predominantly within the mantle range. The data from the Cascade Range and Aleutian Arcs fall within or lower than the typical mantle $\delta^{13}C$ range (**Table S2**). These arcs release He with R/R_A values that also fall consistently within the mantle range. It has been proposed that the low $\delta^{13}C$ is the result of contamination by a shallow sedimentary, likely organic carbon, source, and that the R/R_A values support previous conclusions that the mantle is

the main source of He (*58, 59*). A recent study has observed a correlation between the $\delta^{13}C$ of volcanic products along the Aleutian arc and organic sediment flux into the subducting slab (*7*).

Controls on carbon isotopic composition of volcanic gases

A number of processes control the carbon isotopic composition of carbon in volcanic gases in arcs, relating to subducted component compositions, subduction and devolatilization processes, magma generation and fluid-rock interaction in the wedge, contamination of primary melts by crust, outgassing of magmas during decompression, and interaction with hydrothermal systems (which may include precipitation of calcite) and biogenic material in the shallow subsurface. In order to frame our arguments in the main paper, we provide additional context for these processes here.

Carbon sources on the downgoing slab are inorganic (limestones and carbonate precipitated during hydrothermal circulation and serpentinization of the downgoing slab) and organic carbon (in sediments). Inorganic carbon has a carbon isotopic composition of ~ 0‰ in the present day, while organic carbon has a composition of -20 to -40‰ (**Figure S2**). There are some global trends between volatile inputs from the subducted slab and the C/S ratio in volcanic gases, which suggest that some arcs show gas geochemistry that is related to the nature of the subducting components and to contamination by overlying crust (*7*).

The depth and extent of slab devolatilization is controlled by the thermal structure of the slab and significant decarbonation cannot occur without aqueous fluid infiltration of the slab (*12, 42*) (*8*). It has been suggested that the thermal structure of subduction zones control the depth, extent and efficiency of decarbonation (*8, 10, 60*) and are therefore important in determining the contribution of subducted carbon to volcanic outgassing flux. However, no strong correlation is found between physical parameters and the $\delta^{13}C$ of arc volcanic gases in this study (**Figure S3**). A positive correlation between upper plate thickness and the $\delta^{13}C$ of arc volcanic CO_2 was identified with a more limited dataset (*61*), but this trend is not replicated here. The fractionation of carbon isotopes that occurs on devolatilisation of the subducted slab is not well understood but experiments on basalts (*62*) would suggest that carbon-bearing fluids generated during devolatilization of the slab would be heavy (^{13}C-enriched), leaving a light (^{12}C-enriched) carbon residue of unknown size on the slab that may return to the deep mantle (*9*). In general, the magnitude and direction of equilibrium stable isotope fractionation of carbon ($^{13}C/^{12}C$) depends upon the speciation of carbon (which controls the bonding environment) and temperature of the reaction. We consider that magnesite and/or calcite vs aqueous CO_2 dominate as the main carbon species under the redox conditions commonly considered for arc systems (*63*).

Crustal contamination of magmas may supply carbon due to partial melting or devolatilization of carbon-bearing sediments in the crust. The isotopic composition of CO_2 produced by decarbonation of carbonate material depends on several factors, including the mode of CO_2 separation, reaction progress and temperature, but as the CO_2-calcite fractionation factor at relevant temperatures (400 – 600°C) ranges from 2.6 to 2.7‰, it is expected that the $\delta^{13}C$ of CO_2 produced on decarbonation will be higher than that of the rock from which it derives (*64, 65*). At volcanoes that are known to be underlain by limestone, attempts have been made to quantify the interaction between carbonate host rock and magma e.g. Popocatepetl (*66*), Vesuvio (*33*). Crustal carbonate assimilation may account for the elevated CO_2 fluxes at Vesuvius (Italy) and Etna (Italy) (*33*), overwhelming the signature from mantle-derived CO_2.

Another factor that can modify the $\delta^{13}C$ of volcanic arc CO_2 is carbon isotope fractionation during degassing (*67*). A carbon isotope fractionation factor has been determined by comparing

the carbon isotopic composition of coexisting melt and vapour phases; this has been done experimentally and through literature compilation and is understood to be about ~2‰ for a wide range of temperatures and pressures (*24*). Therefore, when CO_2 degasses from a basaltic melt, the residual melt will be relatively enriched in the light isotope (^{12}C) and the gas will be relatively enriched in the heavy isotope (^{13}C). Assuming closed system degassing of a magma batch, it is therefore possible for the volcanic gases to be maximum 2‰ higher in $\delta^{13}C$ than the degassed melt. However, owing to the low solubility of carbon in silicate melts, most magmas will degas efficiently and almost completely, resulting in the gas phase ending up with the same $\delta^{13}C$ as the original host magma by the mid-upper crust. The effect of degassing on the $\delta^{13}C$ of CO_2 released at volcanoes has been observed on short timescales, however, related to the progressive degassing of single magma batches, and has been shown to correlate with an increase in volcanic activity. For example, An increase in the δ13C of gases released at Etna over time has been concurrent with an increase in eruptive activity and a change in magma composition (*68*). After a large pulse in sulfur and carbon dioxide outputs from Mount Baker in 1975, the $\delta^{13}C$ of CO_2 released was observed to decrease (*69*). This is consistent with progressive, Rayleigh-process CO_2 loss from a cooling intrusion (*67*). A lower $\delta^{13}C$ in volcanic gases at the East Rift zone of Kilauea than in gases emitted from summit fumaroles has been interpreted to be due to progressive, fractional degassing during magma transport from the summit to the rift (*67*).

The loss of CO_2 from geothermal fluids via calcite precipitation can impact the measured and reported $\delta^{13}C$ of volcanic arc CO_2. The carbon isotope fractionation associated with calcite precipitation is temperature dependent. At temperatures <192°C and at high rates of precipitation calcite is enriched in ^{13}C relative to the residual dissolved CO_2, whereas, >192°C the direction of fractionation is reversed (*70*). The magnitude of the carbon isotope fractionation at these temperatures, however, is less than 0.1‰ therefore is unlikely to impact our reported dataset.

Estimates of the fraction of buried organic carbon

We calculate the volcanic gas $\delta^{13}C$ input required to produce the excursions to the high Neoproterozoic $\delta^{13}C_{carb}$ (shown in **table S5**). The volcanic gas $\delta^{13}C$ input is calculated for a range of fractional organic carbon burial values (f_{org}) and for carbon isotope fractionation factors between organic and carbonate carbon of 25‰ and 27‰. It is unlikely that a high $\delta^{13}C$ of volcanic CO_2 alone can account for excursions to $\delta^{13}C_{carb}$ as high as +10‰ because the $\delta^{13}C$ input required to produce such values is unreasonable in the context of the highest $\delta^{13}C$ of volcanic CO_2 released today. However, at higher f_{org} (>0.15) the $\delta^{13}C$ of the volcanic input required for excursions to $\delta^{13}C_{carb}$ = +5‰ is more reasonable, at 0 ± 1 ‰.

Fig. S1.

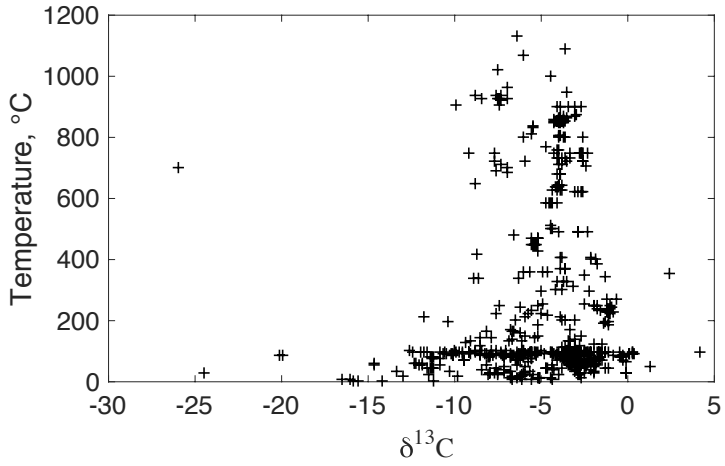

Sample temperature plotted against volcanic gas carbon isotopic composition. There is no correlation between temperature and carbon isotopic composition above 200 °C. There is a suggestion that at temperatures less than 200 °C the data are shifted to lower $\delta^{13}C$, which does not affect our arguments in the main paper.

Fig. S2.

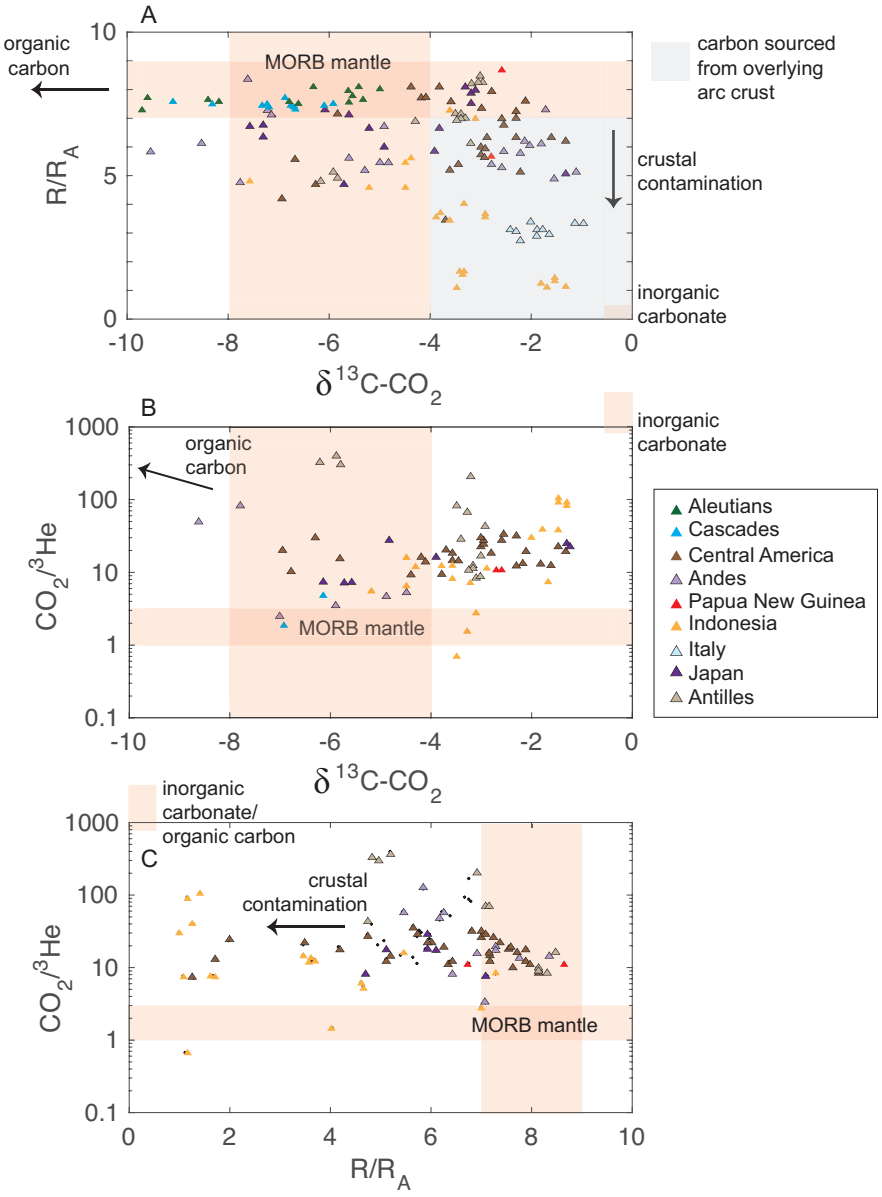

Carbon and helium isotope systematics of the volcanic arc gases considered in this paper, after (*21*), with the reservoirs MORB mantle, organic carbon and inorganic limestone marked. A: R/R_A plotted against $\delta^{13}C$ of volcanic gas CO_2; B: $CO_2/^3He$ plotted against $\delta^{13}C$ of volcanic gas CO_2 and C: $CO_2/^3He$ plotted against R/R_A.

Fig. S3

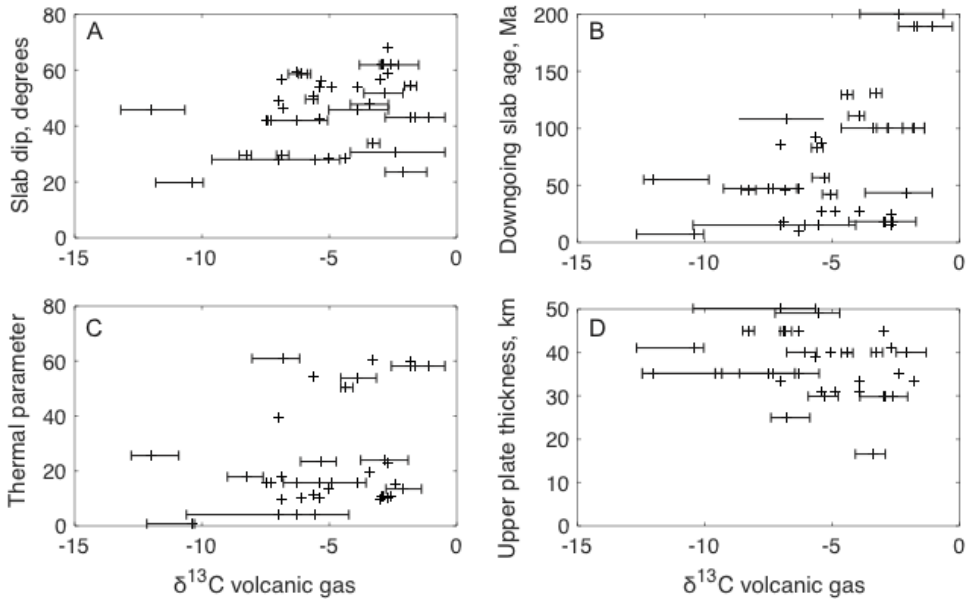

Mean carbon isotopic composition ($\delta^{13}C$) of volcanic CO_2 gas plotted against various subduction parameters showing that physical structure of the subduction zone does not correlate with the carbon isotope composition of the gas. Horizontal lines represent the range in $\delta^{13}C$ at each location. A: Slab dip angle; B: age of the downgoing slab, Ma; C: thermal parameter, equal to the product of plate age, convergence velocity, and the sine of the slab dip angle; D: thickness of the upper plate in km. Subduction zone data from (*60*).

Fig. S4

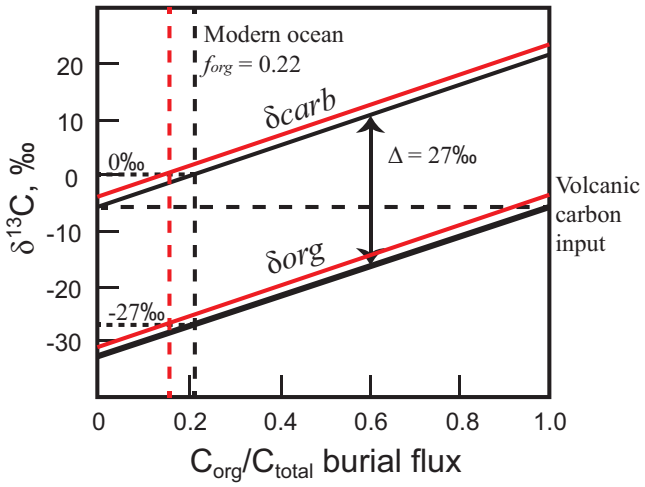

Visual representation of the carbon isotope mass balance equation when using the canonical carbon input value of -5.5 ‰ (black lines), giving an f_{org} of 0.22, or 22%. Red lines: the carbon isotope mass balance when the input is -4.1 ‰ (from **table S4**, assuming arcs release 50% of the global volcanic CO_2 flux); this yields a lower f_{org} of ~0.15, or 15%.

Table S1. (*see also separate excel spreadsheet*)

Data compiled from the literature for carbon and helium isotopic composition of volcanic gases in arcs.

F = fumarolic gas
FC = fumarolic condensate
FwC = fumarole within caldera
SF = summit fumarole
FF = flank fumarole
SolF = solfatara fumarole
P = plume
Calc = plume/crater gas values extrapolated back to remove atmospheric component
G = gas (type not specified)
SG = soil gas
FG = fumarole gas

Arc, country	*Volcano*	*Date*	*Sample type*	*Sample temp (°C)*	*$\delta^{13}C$-CO_2 (‰)*	*R/R_A*	*$CO_2/^3He$ ($x10^9$)*	*$\delta^{15}N$ (‰)*	*Source*
Kermadec									
New Zealand									
	White Island	10/02/98	F		-2.0	6.1			(*71*)
		10/02/98	F		-2.0				
		11/02/98	F		-2.1				
		10/02/98	F		-2.6	5.3			
		10/02/98	F		-4.2				
		11/02/98	F		-3.6				
		1974	G	200	-3.1				(*61*)
Mean (Kermadec)					*-2.8*	*5.7*			
Standard deviation (Kermadek)				*0.9*	*0.6*				
Median (Kermadec)				*-2.6*	*5.7*				
Kuril-Kamchatka									
Russia	Tolbachik	1976	G	1020	-7.5				(*61*)
	Avachinsky	12/09/94	F	472	-5.2				(*72*)
		23/02/91	F	101	-6.1				
	Kudryavy		F	920	-7.3	6.76	87	3.7	(*73*)
			F	710	-7.3	6.36	53	1.6	
			F	690	-7.6	6.73	165	1.1	
			F	480	-6.6				
			F	187	-5.2	6.66	93	2.8	
		1990	FC	770	-4.7				(*74*)
		1990	FC	511	-4.5				
		1990	FC	430	-5.2				
		1990	FC	160	-6.2				
Mean (Kur-Kam)					*-6.1*	*6.63*			
Standard deviation (Kur-Kam)				*1.1*	*0.18*				
Median (Kur-Kam)					*-6.2*	*6.70*			
Japan	Usu		G	586	-4.7				(*75*)

Arc, country	*Volcano*	*Date*	*Sample type*	*Sample temp (°C)*	*$\delta^{13}C$-CO_2 (‰)*	*R/R_A*	*$CO_2/^3He$ ($x10^9$)*	*$\delta^{15}N$ (‰)*	*Source*
			G	586	-4.6				
			G	586	-4.1				
			G	586	-4.4				
			G	586	-4.4				
	Kusatsu-Shirane		G	102	-3.3	8.1			(*32*)
			G	50	-3.2	7.87			
			G	76	-3.8	6.65			
			G	95	-3.1	8.01			
			G	95	-3.2	7.49			
	Oshima		FwC	93	-1.3	5.08	24		(*21*)
	Kuju		F	120	-8.5				(*76*)
			F	340	-8.9				
	Unzen		G	803	-6.1	7.29	8.05		(*31*)
			F	810	-5.6	7.13	7.74		(*21*)
			F	95	-5.7	4.69	7.99		
	Ebino		FwC	96	-3.9	5.87	17.5		(*21*)
	Shinmoe		FwC	>110	-4.9	5.98	27.9		(*21*)
	Satsuma-Iojima	1974	G	836	-5.5				(*61*)
			G	835	-5.5				(*76*)
			G	247	-5.2				
			G	144	-5.4				
Mean (Japan)					*-4.8*	*6.74*			
Standard deviation (Japan)				*1.7*	*1.19*				
Median (Japan)					*-4.6*	*7.13*			
Indonesia									
Java/E.Sunda /Banda	Krakatoa		G	687	-7.0				(*77*)
	Merapi	1989	G	500	-4.4	5.62	14		(*78*)
		1989	G	500	-4.5	5.49	16.1		
	(Woro)	1977	G	680	-3.9				(*79*)
		1977	G	680	-4.1				
		1977	G	680	-3.9				
		1978	G	630	-3.9				
		1978	G	630	-4.1				
		1978	G	644	-4.0				
		1978	G	644	-3.8				
		1978	G	644	-4.0				
		1979	G	630	-4.4				
		1979	G	630	-3.8				
		1979	G	640	-4.0				
		1979	G	640	-4.2				
		1979	G	640	-4.0				
	(Gendol)	1977	G	870	-3.7				
		1977	G	870	-3.1				

Arc, country	*Volcano*	*Date*	*Sample type*	*Sample temp (°C)*	*$\delta^{13}C$-CO_2 (‰)*	*R/R_A*	*$CO_2/^3He$ ($x10^9$)*	*$\delta^{15}N$ (‰)*	*Source*
		1978	G	730	-4.0				
		1978	G	730	-3.3				
		1978	G	730	-3.8				
		1978	G	730	-3.6				
		1978	G	730	-4.1				
		1978	G	801	-3.6				
		1978	G	801	-3.7				
		1979	G	709	-3.8				
		1979	G	709	-4.0				
		1979	G	758	-4.1				
		1979	G	758	-4.0				
		1979	G	804	-4.0				
		1979	G	804	-3.9				
		1979	G	850	-3.7				
		1979	G	850	-4.0				
		1979	G	850	-4.3				
		1979	G	850	-3.9				
		1979	G	853	-3.7				
		1979	G	853	-4.1				
		1979	G	853	-4.2				
		1979	G	853	-4.1				
		1979	G	853	-4.3				
		1979	G	853	-4.1				
		1979	G	853	-3.8				
		1979	G	853	-4.0				
		1979	G	853	-4.1				
		1979	G	853	-4.0				
		1979	G	853	-3.8				
		1979	G	853	-3.8				
	(Dome)	1978	G	863	-4.0				
		1978	G	863	-3.9				
		1978	G	863	-3.5				
		1978	G	863	-3.9				
		1978	G	901	-4.1				
		1978	G	901	-3.1				
		1978	G	901	-3.4				
		1979	G	860	-4.0				
		1979	G	860	-4.0				
		1979	G	860	-3.7				
		1979	G	860	-4.3				
	Egon		G	124	-1.5	1.27	39.1		(*78*)
			G	124	-2.0				
			G	98	-1.8	1.23	39.7		
	Lewotolo	1984	G	490	-2.9	3.62	11.9		
		1984	G	490	-2.9	3.57	12.0		
			G	96	-3.5				
			G	96	-3.7				

Arc, country	*Volcano*	*Date*	*Sample type*	*Sample temp (°C)*	*$\delta^{13}C\text{-}CO_2$ (‰)*	*R/R_A*	*$CO_2/^3He$ ($x10^9$)*	*$\delta^{15}N$ (‰)*	*Source*
			G	200	-3.6				
			G	200	-3.8				
			G	214	-3.9				
			G	300	-4.2				
			G	300	-3.8	3.67	12.6		
			G	330	-3.7				
			G	330	-4.1				
			G	330	-3.5				
			G	360	-4.9				
			G	360	-5.7				
			G	360	-4.6				
			G	372	-3.6	3.47	14.6		
			G	372	-3.6				
			G	372	-3.9				
			G	406	-3.8	3.61	11.8		
			G	406	-3.9				
			SF	n.d.	-2.9	3.62	13.4		(*80*)
	Sirung	1984	G	95	-1.7				(*78*)
			G	95	-1.7	1.07	7.9		
	Wurlali	1984	FF	135	-3.4	1.69	7.9		(*80*)
		1984	SF	170	-3.3	1.65	7.6		
Sangihe	Awu		CF	96.6	-2.0	1.00	31.2		(*52*)
			CF	96.6	-1.5	1.39	108		
			CF	96.6	-1.3	1.14	96		
	Ruang		SolF	97.9	-3.3	4.02	1.49		
			SolF	140	-3.1	6.99	2.83		
	Lokon		F	96.1	-3.6	7.27	8.4		
	Soputan		F	72.9	-3.5	1.11	0.69		
	Ambang		SF	97.6	-5.2	4.64	5.7		
			SF	97.6	-4.5	4.60	6.45		
Mean (Indonesia)					*-3.7*	*3.26*			
Standard deviation (Indonesia)				*0.8*	*1.96*				
Median (Indonesia)					*-3.9*	*3.59*			
Papua New Guinea									
(Rabaul)	Tavurvur		F	99	-2.6	8.64	11.2		(*31*)
	Rabalanakaia		F	99	-2.8	5.71	11.4		
Mean (PNG)					*-2.7*				
Standard deviation (PNG)				–					
Median (PNG)					*-2.7*				
Lesser Antilles									
Montserrat	Soufrière Hills	27/02/96	G	720	-5.9				(*81*)
		27/02/96	G	150	-5.2				
St Lucia	Qualibou		SF	67.7	-5.8	4.92	313.6		(*56*)
			SF	51.5	-5.9	5.20	405.8		

Arc, country	*Volcano*	*Date*	*Sample type*	*Sample temp (°C)*	*$\delta^{13}C\text{-}CO_2$ (‰)*	*R/R_A*	*$CO_2/^3He$ ($x10^9$)*	*$\delta^{15}N$ (‰)*	*Source*
			SF	77.7	-6.2	4.84	329.9		
Dominica	Valley of Desolation		SF	71.6	-3.5	6.79	83.8		
			SF	57.7	-3.4	7.12	28.4		
			SF	61.8	-3.3	7.10	69.7		
			SF	61.8	-3.2	6.91	201.6		
			SF	53.1	-3.3	7.14	69.2		
			SF		-2.93	4.73	43.5		(*57*)
Guadeloupe	La Soufrière		SF	94	-3.2	7.94	11.5		(*56*)
			SF	94	-3.1	7.96	11.6		
			SF		-3.01	8.32	8.9		(*56*)
			SF		-3.02	8.46	17.1		
		May 2007	SF		-3.17	7.9	12		(*82*)
		Oct 2010	SF		-3.21	8.2	9		
	Saint Vincent		G	45053.1	-5.61				(*83*)
			G	450	-5.25				
			G	450	-5.37				
			G	450	-5.37				
			G	450	-5.51				
Mean (Antilles)					*-4.3*	*6.90*			
Standard deviation (Antilles)				*0.5*	*1.34*				
Median (Antilles)					*-3.5*	*7.12*			
Aleutians									
(Arc)	Kanaga		P		-5.0				(*84*)
			P		-4.9				
			P		-5.9				
			P		-6.3				
			P		-5.0				
			P		-5.0				
			P		-5.4				
			F	94.5	-5.6				
	Makushin	24/07/96	FF	100	-7.6	4.81			(*59*)
	Akutan	29/07/96	SF	96.6	-12.0	7.24			
		28/07/96	FF	97.8	-9.7	7.26			
(Range)	Augustine	Jul 1979	SF	648	-8.8				(*85*)
		Jul 1979	SF	746	-9.2				
		Jul 1979	SF	746	-7.7				
		Jul 1979	SF	721	-7.7				
		Jul 1979	SF	338	-8.6				
		Aug 1982	SF	472	-5.6	7.6			
		Aug 1982	SF	472	-5.2				
		28/07/94	SF	97	-5.4	8.06			(*59*)
		19/07/08	SF	98	-5.54	7.79			
		19/07/08	SF	98	-5.34	7.68			
		27/07/10	SF	94.1	-5.94				

Arc, country	*Volcano*	*Date*	*Sample type*	*Sample temp (°C)*	*$\delta^{13}C$-CO_2 (‰)*	*R/R_A*	*$CO_2/^3He$ ($x10^9$)*	*$\delta^{15}N$ (‰)*	*Source*
		27/07/10	SF	94.1	-5.98				
		27/07/10	SF	92.4	-5.96				
	Griggs	22/07/95	SF	93.8	-6.3	8.11			
		16/07/98	SF	93.1	-6.3	8.12			
		22/07/95	FF	99.8	-5.0	8.04			
		18/07/97	FF	99.2	-5.6	7.94			
		16/07/98	FF		-5.1			4.3	
	Mageik	26/07/95	SF	167.4	-6.6	7.48			
		19/07/97	SF	172.9	-6.8	7.57			
		22/07/98	SF	101.6	-8.4	7.64		2.1	
		22/07/98	SF	166.6	-8.2	7.61		2.5	
	Trident	13/0794	FF	93.9	-10.2	7.48			
		24/07/95	FF	94.2	-10.1	7.66			
		17/07/97	FF	94.2	-10.5	7.82			
		18/07/98	FF	94	-9.6	7.69		3.2	
Mean (Aleutians)					*-7.0*	*7.56*			
Standard deviation (Aleutians)				*2.0*	*0.71*				
Median (Aleutians)					*-6.3*	*7.66*			
Cascades									
	Baker	10/06/94	SF	135	-6.1	7.42			(*59*)
		06/09/94	SF	150	-5.9	7.49			
		23/08/96	SF	137	-6.7	7.45			
		23/08/96	SF		-6.1				
		07/08/97	SF	134.4	-6.9	7.70		1.9	
		07/08/97	SF		-6.1			4.8	
		2006	SF		-6.7	7.36			(*69*)
		2006	SF		-6.7	7.31			
		2007	SF		-7.3	7.44			
		2007	SF		-7.2	7.48			
		2007	SF		-7.2	7.34			
	Mt St Helens	16/08/80	P		-10.2				(*86*)
		16/08/80	P		-9.5				
		20/08/80	P		-9.1				
		23/08/80	P		-10.2				
		23/08/80	P		-8.4				
		24/08/80	P		-8.8				
		04/11/80	F	93	-10.7				
		04/11/80	Crack	>400	-10.5				
			SF	≥86	-11.8				(*87*)
			SF	≥85	-12.0				
		29/06/98	SF		-11.9				(*59*)
	Hood	23/06/95	SF		-8.3	7.48			
		08/10/96	SF		-9.6				
		09/10/96	SF	91	-9.8				
		09/09/97	SF		-9.1	7.60			

Arc, country	*Volcano*	*Date*	*Sample type*	*Sample temp (°C)*	*$\delta^{13}C$-CO_2 (‰)*	*R/R_A*	*$CO_2/^3He$ ($x10^9$)*	*$\delta^{15}N$ (‰)*	*Source*
Mean (Cascades)					*-8.6*	*7.46*			
Standard deviation (Cascades)				*2.0*	*0.11*				
Median (Cascades)					*-8.6*	*7.45*			
Central America									
(Mexico)	Colima		F	340	-6.29	4.72	28.1		(*31*)
(Guatemala)	Zunil		F	94	-2.86	6.32	11.4		
	Pacaya		G	965	-6.94	4.17	19.7		
		01/03/92	FC	84.5 (240)	-2.8	7.91	18		(*88*)
	Teacuam-burro	01/03/89	FC	95 (110)	-3.0	5.96	29		
(El Salvador)	Cuyanaul		FF	95.1	-2.3	6.37	12.1		(*89*)
			FF	97.4	-1.6	6.38	12.2		
	Santa Ana		SF	400	-2.1	7.56	19.2		
			SF	875	-3.0	7.37	22.1		
	San Vicente		FF	97.8	-1.3	6.24	19.3		
	Chinameca	Aug 1999	FC		-3.70	3.47	21		(*88*)
		Aug 1999	FC	(153)	-2.98	5.95	24.8		
	Meanguera		FF	98.6	-2.2	5.11	13.2		(*89*)
			FF*(dup)*	98.6	-3.6	5.19	14.8		
(Nicaragua)	San Cristobal		SF	95.6	-2.9	5.65	38		(*51*)
			SF *(dup)*	95.6	-3.0	5.74	26		
	Cerro Negro		SF	310	-3.2	1.26	7.4		
			SF	386	-1.8	1.72	13.1		
			SF	97.7	-2.3	6.99	31		
			F	350	-2.54	6.8	33.3		(*31*)
			SF		-3.02				(*90*)
	Momotombo		SF	747	-2.6	6.99	27		(*51*)
			SF*(dup)*	747	-2.6				
			F	748	-3.3				(*91*)
			F	748	-2.7				
			F	748	-2.3				
			F	748	-2.7				
			F	748	-4.3				
			F	748	-2.8				
			F	720	-3.5				
			F	720	-2.6				
			F	720	-2.6				
			F	623	-2.7				
			F	623	-2.6				
			F	623	-2.9				
			F	623	-3.1				
			F	490	-2.3				
			F	490	-4.0				
	Masaya		FF	72.5	-1.5	1.98	23		(*51*)

Arc, country	*Volcano*	*Date*	*Sample type*	*Sample temp (°C)*	*$\delta^{13}C$-CO_2 (‰)*	*R/R_A*	*$CO_2/^3He$ ($x10^9$)*	*$\delta^{15}N$ (‰)*	*Source*
	Mombacho		SF	110.4	-3.1				
			SF*(dup)*	110.4	-3.6	7.6	17.8		
(Costa Rica)	Arenal	1979	G	900	-2.7				(*61*)
	Poás		F	95	-3.44	5.38	14.4		(*31*)
			SF	76	-5.6				(*51*)
			SF	76		7.10	15.9		
			SF*(dup)*	76		6.90	15.4		
			SF	92.2		7.22	12.4		
			SF*(dup)*	92.2	-6.8	7.60	9.9		
			SF	92.2	-5.8	7.14	15.3		
	Irazú		FF	88.5	-2.3				
			FF*(dup)*	88.5	-2.3	7.24	27		
	Turrialba		SF	89.6	-3.3				
			SF*(dup)*	89.6	-4.1	7.74	14.3		
			SF	89.7	-4.4	8.1	9.8		
			SF*(dup)*	89.7	-3.8	8.1	9.4		
			SF	84.2	-4.2	7.7	16.1		
Mean (CAVA)					*-3.2*	*6.15*			
Standard deviation (CAVA)				*1.2*	*1.81*				
Median (CAVA)					*-2.9*	*6.80*			
Andes									
(Colombia NAVZ)	Cumbal	14/08/96		167	-6.7	5.56			(*92*)
		14/08/96		233	-5.6	5.60			
		14/08/96		299	-5.0	5.51			
				257	-4.92	6.75	11.7		(*31*)
	Galeras		G	225	-5.8				(*93*)
			G	243	-6.2				
			G		-7.4			2.7	
			G	249	-7.4			2.7	
			G	218	-4.6			5.3	
			G	213	-5.9			0.1	
			G	222	-5.0			4.7	
			G	358	-6.0			3.6	
			G	197	-10.4			2.7	
			G	145	-8.5				
			G	416	-8.7			57.2	
			G	145	-7.9			93.4	
			F	222	-7.61	8.35	15.2		(*31*)
	Purace	06/08/90	SF	86	-8.5	7.15			(*94*)
	Machin		F	96	-9.54	5.82	31.2		(*31*)
Mean (Colombia)					*-6.9*	*6.39*			
Standard deviation (Colombia)				*1.7*	*1.08*				
Median (Colombia)					*-6.7*	*5.82*			
(N Chile CAVZ)	Tacora		F	93	-4.84	5.41			(*95*)
			F	89.1	-5.29	5.20			

Arc, country	*Volcano*	*Date*	*Sample type*	*Sample temp (°C)*	*$\delta^{13}C$-CO_2 (‰)*	*R/R_A*	*$CO_2/^3He$ ($x10^9$)*	*$\delta^{15}N$ (‰)*	*Source*
	Irruputuncu		F	89	-7.23	7.27	18.8		(*96*)
			F	202	-6.53				
	Olca		F	91	-8.54	6.11	17.2		
			F	84	-8.04				
	Putana		F	82	-6.74				
			F	83	-7.11	7.14	17.4		
	Alitar (Maar)		F	85	-7.75	4.8	40.4		
			F	85	-8.01				
	Lascar	May 2005	F	76		7.08	3.19		(*97*)
		Oct 2006	F	71.9		6.4	8.35		
		Oct 2006	F	73.2	-3.34				
		Oct 2006	F	150.8	-2.71				
		Oct 2006	F	250	-1.74	7.3	16.6		
	Lastarria	May 2006	G	85	-4.13				(*98*)
		May 2006	G	95	-2.72				
		March 2008	G	120	-2.77	5.44	60		
		April 2009	G	345	-1.33				
			G	295	-2.22	5.75	33		
		June 2009	G	400	-1.82	6.17	46		
		Mar 2008	G	95	-1.11	5.11	18		
		May 2006	G	81	-1.55	4.93	20		
		May 2006	G	81	-2.83				
		May 2006	G	81	-0.42				
		Apr 2009	G	408	-2.14	6.23	59		
		Mar 2008	G	254	-2.55	5.83	120		
Mean (N Chile)					*-4.14*	*6.01*			
Standard deviation (N Chile)				*2.60*	*0.84*				
Median (N Chile)					*-2.83*	*5.97*			
Mean (Andes)					*-5.3*	*6.13*			
Standard Deviation (Andes)				*2.6*	*0.92*				
Median (Andes)					*-5.7*	*5.83*			
Aegean									
	Nisyros	Nov 1999	SF		-3.34				(*99*)
		Nov 1999	SF		-1.94				
		Nov 1999	SF		-2.32				
		Nov 1999	SF		-4.08				
		Nov 1999	SF		-3.21				
		Nov 1999	SF		-1.44				
		Nov 1999	SF		-2.09				
		Nov 1999	SF		-0.40				
		Nov 1999	SF		-2.46				
Mean (Aegean)					*-2.36*				
Standard deviation (Aegean)				*1.09*					

Arc, country	*Volcano*	*Date*	*Sample type*	*Sample temp (°C)*	*$\delta^{13}C$-CO_2 (‰)*	*R/R_A*	*$CO_2/^3He$ ($x10^9$)*	*$\delta^{15}N$ (‰)*	*Source*
Median (Aegean)					*-2.32*				
Italy									
	Solfatara		Calc		-1.68				(*68*)
			Calc		-1.72				
			Calc		-1.87				
			Calc		-2.34				
	Vesuvio	24/06/98	SF	96.3	0.24				(*100*)
		14/11/98	SF	94	0.06				
		24/06/98	SF	93.7	0.24				
		14/11/98	SF	94	0.12				
		24/06/98	SF	97.8	0.29				
		14/11/98	SF	94.5	0.34				
	Stromboli	30/01/02	SF		-2.0	3.36			(*101*)
		13/03/02	SF		-2.3	3.09			
		09/04/02	SF		-1.6	2.93			
		17/06/02	SF		-1.9	2.92			
		22/07/02	SF		-1.8	3.12			
		19/10/02	SF		-1.1	3.35			
		20/11/02	SF		-1.0	3.34			
		11/12/02	SF		-1.7	2.99			
		14/01/03	SF		-2.2	2.77			
		20/01/03	SF		-2.3	3.04			
		03/02/03	SF		-2.4	3.12			
	Vulcano		Calc		-1.70				(*102*)
			Calc		-1.94				
			Calc		-1.89				
			Calc		-1.84				
			Calc		-1.68				
			Calc		-1.27				
			Calc		-1.18				
	Etna		Calc		-0.94				(*103*)
			Calc		-1.03				
			Calc		-1.07				
			Calc		-1.01				
			Calc		-1.01				
			Calc		-0.33				
			Calc		-1.44				
			Calc		-1.50				
			Calc		-1.37				
			Calc		0.25				
			Calc		1.46				
			Calc		-0.85				
			Calc		-0.43				
			Calc		0.09				
			Calc		-0.95				
			Calc		-0.67				
			Calc		-0.60				

Arc, country	*Volcano*	*Date*	*Sample type*	*Sample temp (°C)*	*$\delta^{13}C\text{-}CO_2$ (‰)*	*R/R_A*	*$CO_2/^3He$ ($x10^9$)*	*$\delta^{15}N$ (‰)*	*Source*
			Calc		-0.20				
			Calc		-0.65				
			Calc		-0.88				
			Calc		-0.40				
			Calc		-1.11				
			Calc		-0.87				
			Calc		-1.32				
			Calc		-1.06				
			Calc		0.91				
			Calc		0.88				
			Calc		0.90				
			Calc		0.91				
			Calc		0.89				
Mean (Italy only)					*-1.1*				
Standard deviation (Italy only)				*0.9*					
Median (Italy only)					*-1.1*				
Mean (Etna only)					*-0.7*				
Standard deviation (Etna only)				*0.6*					
Median (Etna only)					*-0.9*				

Table S2.

Data compiled from the literature for carbon and helium isotopic composition of volcanic gases in non-convergent settings.

Tectonic setting	*Volcano*	*Sample type*	*Sample Temperature (°C)*	*$\delta^{13}C$-CO_2 (‰)*	*Citation*
Intra-continental hotspot	Yellowstone	FG		-3.2	(*40*)
		FG		-4.8	
		FG		-4.2	
		FG		-2.5	
		FG		-3.2	
		FG		-4.9	
		FG		-3.9	
		SG		-4.9 to -2.3	
		Mean, stdev		-3.8 +/- 0.9	
East African Rift	Ol Doinyo Lengai	FG		-7.4	(*104*)
		FG		-4.5	
		FG		-2.6	
		SG		-0.8	
		SG		-0.4	
		SG		0.3	
		SG		-2.4	
		SG		-2.7	
		SG		-2.2	
	Ardoukoba	G	1070	-6.0	(*61*)
	Erta Ale	G	1130	-6.4	
Incipient rift	Erebus	SG	45.3	-3.7	(*105*)
		SG	51.2	-3.8	
		SG	61.9	-3.4	
		SG	35.9	-4.3	
		SG	32.9	-3.7	
		Fumarolic ice tower/cave	6.0	-2.1	
		Fumarolic ice tower/cave	11.8	-3.5	
		Fumarolic ice tower/cave	11.5	-4.7	
		Fumarolic ice tower/cave	1.3	-6.7	
		Fumarolic ice tower/cave	-0.5	-4.1	
		Fumarolic ice tower/cave	-1.7	-4.4	
Rift (mid-Atlantic)	Iceland	Calculated parental magma value	n/a	-2.5±1.1	(*106*)
	Iceland – Western rift zone	G	89	-4.69	
		G	89	-2.59	
		G	100	-3.4	
		G	100	-2.99	
		G	99.6	-3.43	

		G	99.6	-3.93	
		G	77.5	-4.23	
		G	77.5	-3.59	
		G	72.8	-3.96	
		G	72.8	-4.45	
		G	77.5	-3.1	
		G	82.6	-2.73	
		G	82.6	-2.66	
		G	94.7	-4.06	
		G	89.6	-5.05	
		G	100.7	-2.36	
		G	100.7	-2.32	
	Eastern rift zone	G	98.6	-3.04	
		G	97.7	1.62	
		G	97.7	1.42	
	Northern rift zone	G	76.5	-4.37	
		G	96.7	-4.78	
		G	96.7	-2.44	
		G		-5.29	
		G		-5.09	
		G	89.9	2.86	
		G	26.8	-3.58	
		G	30.5	-4.19	
		G		-2.43	
		G		-1.98	
Intra-oceanic hotspot	Kilauea, Hawaii	Calculated parental magma value	n/a	-4.1 to -3.4	(*67*)

Table S3.

Flux-weighted mean and median of the global volcanic arc carbon isotopic composition of CO_2 released from volcanoes. Due to the dominance of the Etnean flux I the overall flux from Italy, the mean Italian isotopic composition is calculated using Etna only. The calculations are speculative as uncertainties on both the isotopic composition and the fluxes are likely to be large. Arcs are listed in order of highest to lowest flux. CO_2 flux is from (*36*), given in units of x 10^9 moles per year. #volcanoes is the number of volcanoes used for the calculation.

Arc	*CO_2 flux*	*Median $\delta^{13}C$ (‰)*	*Mean $\delta^{13}C$ (‰)*	*Standard deviation*	*#volcanoes*
Papua New Guinea	505.96	-2.7	-2.7	0.12	1
Italy (Etna)	482.43	-0.8	-0.7	0.98	1
Andes	312.85	-5.7	-5.3	2.63	11
Central America	72.42	-2.9	-3.2	1.22	17
Kermadec	58.01	-2.6	-2.8	0.87	1
Japan	52.20	-4.6	-4.8	1.69	8
Antilles	14.99	-3.5	-4.3	1.26	5
Indonesia	9.43	-3.9	-3.7	0.82	11
Kuril-Kamchatka	1.53	-6.2	-6.1	1.14	3
Aleutians	0.11	-6.3	-7.0	1.94	8
Total arcs	*1510*				
Global (+20.6%)	*1931*				

Table S4.

Calculations of the global mean volcanic $\delta^{13}C$ and how it varies with assumptions about un-sampled arcs and proportion of global volcanic CO_2 from arcs. Calculations use the flux-weighted median $\delta^{13}C$ for the arcs which have measurements associated with them, from Table S1. *CO_2 from arcs* shows the proportion of global CO_2 emitted from arc volcanoes as a percentage, with citations given next to the estimates. Global mean volcanic $\delta^{13}C$ assumes mid-ocean ridge and intra-oceanic hotspot $\delta^{13}C$ = -5.0‰. The range in the global mean volcanic gas *$\delta^{13}C$* reflects the uncertainty in the estimate.

Calculation	*Mean arc $\delta^{13}C$ (‰)*	*% global CO_2 from arcs*	*Global mean $\delta^{13}C$ (‰)*
Assuming un-sampled arcs $\delta^{13}C$ = -3.0‰	-2.8 ± 0.5	63	-3.8
	-2.8 ± 0.5	33 (*39*)	-4.6
Assuming un-sampled arcs $\delta^{13}C$ = -5.0‰	-3.3 ± 0.5	50 (*31*)	-4.1

Table S5.

Example calculations to show the volcanic input values required to produce carbonate isotopic compositions during the Neoproterozoic (of between +5 and +10‰). Fractional organic carbon burial values are varied between 0.10 and 0.22, calculated for a constant offset of 25 and 27‰. Grey-shaded values are rarely measured in volcanic gases today and are therefore considered unreasonable; therfore, a heavy carbon volcanic input is unlikely to be able to explain carbonate compositions as heavy as +10‰.

Carbonate $\delta^{13}C$	*+5‰*		*+10‰*	
f_{org}	Δ = 25‰	Δ = 27‰	Δ = 25‰	Δ = 27‰
0.10	+2.5	+2.3	+7.0	+6.8
0.11	+2.3	+2.0	+6.7	+6.5
0.12	+2.0	+1.8	+6.4	+6.2
0.13	+1.8	+1.5	+6.1	+5.8
0.14	+1.5	+1.2	+5.8	+5.5
0.15	+1.3	+1.0	+5.5	+5.2
0.16	+1.0	+0.7	+5.2	+4.9
0.17	+0.8	+0.4	+4.9	+4.6
0.18	+0.5	+0.1	+4.6	+4.2
0.19	+0.3	-0.1	+4.3	+3.9
0.20	+0.0	-0.4	+4.0	+3.6
0.21	-0.3	-0.7	+3.7	+3.3
0.22	-0.5	-0.9	+3.4	+2.9